QUARTERLY OF APPLIED MATHEMATICS
VOLUME LXXV, NUMBER 4
DECEMBER 2017, PAGES 737–767
http://dx.doi.org/10.1090/qam/1477
Article electronically published on July 20, 2017

COMPOSITIONAL FLOW IN POROUS MEDIA: RIEMANN PROBLEM FOR THREE ALKANES

By

VÍTOR MATOS (*Centro de Matemática, Faculdade de Economia, Universidade do Porto*
Rua Dr. Roberto Frias
4200-464 Porto, Portugal)

AND

DAN MARCHESIN (*Instituto Nacional de Matemática Pura e Aplicada (IMPA)*
Estrada Dona Castorina 110
22460-320 Rio de Janeiro, RJ, Brazil)

Abstract. We consider the flow in a porous medium of three fluid compounds such as alkanes with different boiling points; the compounds partition into a liquid and a gaseous phase. Under some judiciously chosen physical assumptions, the flow is governed by a system of conservation laws; we derive the expression for the Rankine-Hugoniot locus, which involves a parameter dependent fifth degree polynomial in two variables. This expression allows us to establish in detail the bifurcation behavior of the locus

Supplemented by the analysis of characteristic speeds and eigenvectors, the bifurcation analysis of the Rankine-Hugoniot locus is the enabling fulcrum for solving the Riemann problem for all data, which should be a prototype for general three component flow of two phases in porous media. Despite the existence of many similarities between this model and earlier models where proofs were not possible, here we managed to prove analytically many features.

This system of conservation laws has three equations yet it leads to a characteristic polynomial of degree two; this peculiar feature has been unveiled recently, and it is typical of flow of fluids that change density upon changing phase.

1. Introduction. In this work we study a system of three conservation laws where the accumulation function depends on two variables while the transport function depends on three variables (the third one is the seepage velocity). This leads to a generalized eigenvalue problem where a 3×3 matrix has only two eigenvalues counting multiplicity;

Received September 12, 2016 and, in revised form, June 14, 2017.
2010 *Mathematics Subject Classification.* Primary 35L65, 76S05, 76T30.
This work was partially supported by CNPq under Grants 402299/2012-4, 304264/2014-8, 470635/2012-6, and 170135/2016-0 as well as supported by FAPERJ under Grants E-26/110.658/2012, E-26/110.114/2013, E-26/201.210/2014, and E-26/210.738/2014.
E-mail address: vmatos@fep.up.pt
E-mail address: marchesi@fluid.impa.br, marchesi@impa.br

thus, there are just two rarefaction fields and only two branches of the Hugoniot curve from a state (Lax's theorem is not applicable here). This implies that left and right states of a Riemann problem are not independent: for instance, given a left state the right state has just two degrees of freedom. Therefore, the Riemann problem may be solved in two independent variables and then the third variable may be obtained from the previous ones. This kind of conservation laws were studied also in [4, 11, 22]; they model porous media transport with variable total volume depending on compositional parameters.

Flow in porous media for two liquids such as petroleum and water is modeled by the Buckley-Leverett scalar conservation law; the solution for the associated injection problem, or Riemann solution, was established in the forties. Often a third chemical component is injected together with the water to change its properties and improve recovery. In some cases, the volume of the fluids (or phases) can be regarded as unchanged. The model involves a system of two conservation laws; its Riemann solution can be found in Engineering textbooks, for example, [9], as well as in the mathematical literature, [5,7,8]. More realistically, transfer of a compound between two phases changes the total volume, and the associated model involves a system of three conservation laws with the unusual property of possessing only two characteristic speeds; yet it has a proper Riemann solution that is the subject of this work.

In our work we study a model which Riemann solution was unknown: how three alkanes flow in a porous media when one of them may move between phases changing the total volume of fluid (under some judiciously chosen physical assumptions). To this problem, we obtain an explicit expression for Rankine-Hugoniot, Eq. (4.4), allowing us to establish just two stable configurations, Theorem 4.17; we classify the shocks studding perturbations of a singular Hugoniot, Subsection 5.1; and we analytically obtain rarefaction fields and codimension-1 structures, Section 3. Probably, we give the most detailed solution for the Riemann problem in this class of conservation laws, despite the seven parameters that model depends on.

Our problem differs from the problems in [5–8, 17] due to the existence of a third variable, named u. The results in [5–8, 17] are related to systems where the characteristic analysis is standard. We mean, such papers refer to standard eigenvalues, $\det(A - \lambda I) = 0$, rather than to generalized ones. Our paper handles a problem of the form $\det(A - \lambda B) = 0$, where B is singular. These kinds of systems began to be studied a few years ago by J. Bruining et al.; see for instance [11]. They have an unbounded eigenvalue due to incompressibility. More precisely, it is common to assume fluid incompressibility without yielding an infinity eigenvalue because the volume is considered constant. Then, the issue is to assume incompressibility and allow fluid volume variations due to chemical reactions, mass exchanging between phases (our case), adsorption, etc. Surprisingly, after a projection (in some way, ignoring u) the solutions of both kinds of problems have so many similarities.

We solve the Riemann problem using Liu's entropy criterion for all pairs of left and corresponding right states, which allows one to verify that the solution depends on L^1_{loc} continuously on left and right states.

In Section 2, we derive the model that is the subject of this paper: the flow in a porous medium of three alkanes with different boiling points. One has vanishing vapor pressure, so it exists only in vapor state, the other one has intermediate vapor pressure and exists in both vapor and liquid form, while the third one has infinite vapor pressure so that it exists only in liquid phase. We think that this model is a good approximation to models in which the three alkanes exist in both phases: the lightest alkane has a lower but non-vanishing vapor pressure in such a way that it dissolves slightly in the liquid phase and the heaviest evaporates in small quantities. Another restriction is that the temperature must stay away from critical value. Our problem differs from the compositional problems studied in [3, 6, 17] since in our case the volume changes with composition variation.

In Section 3, we determine quantities important for the analysis of Riemann solutions: the eigenvalues, eigenvectors, coincidence locus, inflection locus, and L-regions.

In Section 4 we study the Hugoniot locus which splits in saturation and evaporation branches. We establish only two stable configurations to the Hugoniot for physical relevant states. Finally, with theoretical and numerical tools, we classify the Hugoniot curve.

In Section 5 we present the solution of Riemann problems for all left and right states in projected physical domain (see Definition 2.5), allowing the verification of the L^1_{loc} continuity of the solution with respect to the Riemann data.

In Appendix A we present some useful results on polynomials.

2. Physical model. We are interested in a porous rock filled by two phases, a gaseous phase and a liquid oleic phase. No chemical reactions occur and the temperature is constant. There are three chemical components, a light gaseous hydrocarbon A, a volatile hydrocarbon B and a non-volatile (or "dead") hydrocarbon D. The light hydrocarbon exists only in the gaseous phase, the volatile hydrocarbon exists both in the liquid and gaseous phases, while the dead oil exists only in the liquid phase. The overall flow is governed by Darcy's law, relating pressure gradients to the flow of the phases.

2.1. *Thermodynamical equilibrium assumptions.* We assume that the temperature (T) is constant and that variations in pressure (P) can be considered negligible as far as thermodynamical properties are concerned.

Let ϱ_o and ϱ_g be the molar concentrations (number of moles per unit volume) of the oleic and gaseous phases, respectively; let ϱ_{gi}, $i \in \{a, b\}$, and ϱ_{oi}, $i \in \{b, d\}$, be the molar concentrations of the respective component i in the gaseous and oleic phase; finally, let y_i be the molar fractions of each component in the oleic phase. In the liquid phase we have, by definition:

$$(i)\ \ \varrho_o = \varrho_{ob} + \varrho_{od}, \quad (ii)\ \ y_b = \varrho_{ob}/\varrho_o, \quad (iii)\ \ y_d = \varrho_{od}/\varrho_o, \quad (iv)\ \ y_b + y_d = 1. \quad (2.1)$$

We use the molar fraction of dead hydrocarbon $y \equiv y_d$ as an independent variable.

2.1.1. *The gaseous phase.* We assume that the ideal gas law holds, so, under constant temperature and pressure, the molar concentration of the gaseous phase is constant irrespectively of the gas mixture composition: $\varrho_G = P/RT$.

Let $P_V = \varrho_v RT$ be the vapor pressure of the pure volatile hydrocarbon B at the current temperature. Let P_{ga} be the partial pressure of hydrocarbon A. From Raoult's

law, the partial vapor pressure of component B is $P_{gb} = P_V\, y_b$ or:

$$P_{gb} = P_V\,(1-y). \tag{2.2}$$

From $P = P_{ga} + P_{gb}$, Eq. (2.2), $P_{ga} = \varrho_{ga} RT$, and $P_{gb} = \varrho_{gb} RT$ we get:

$$(i)\ \varrho_{ga}(y) = \varrho_g - \varrho_v\,(1-y)\,, \quad (ii)\ \varrho_{gb}(y) = \varrho_v\,(1-y)\,. \tag{2.3}$$

The model has non-negative molar concentration $\varrho_{ga}(y)$ for $y \geq 1 - \varrho_g/\varrho_v$. Therefore, if $\varrho_g \geq \varrho_v$ the model is meaningful for all $y \in [0,1]$.

The gas viscosity, μ_g, is considered constant.

2.1.2. *The oleic phase.* Let ϱ_b and ϱ_d denote the molar concentrations of B (volatile) and D (dead) pure hydrocarbons at the prevailing temperature and pressure. Consider the molar volumes $\nu_b = 1/\varrho_b$ and $\nu_d = 1/\varrho_d$.

In an ideal liquid mixture the volume is preserved, that is, mixing a volume V_B of liquid pure component B to a volume V_D of liquid pure component D we get a total volume $V_T = V_B + V_D$; *i.e.*, the volume neither increases nor decreases. The moles of component B in the volume V_B are $m_B = \varrho_b V_B$; similarly, $m_D = \varrho_d V_D$. The molar concentration of the mixture is (note that we are using the volume conservation):

$$\varrho_o = \frac{m_B + m_D}{V_T} = \frac{m_B + m_D}{\frac{m_B}{\varrho_b} + \frac{m_D}{\varrho_d}} = \frac{\varrho_b\,\varrho_d}{\frac{m_B}{m_B+m_D}\,\varrho_d + \frac{m_D}{m_B+m_D}\,\varrho_b}; \tag{2.4}$$

using $y \equiv y_d = m_D/(m_B + m_D)$ and $1 - y = m_B/(m_B + m_D)$ on Eq. (2.4) we get the molar concentration of the oleic phase:

$$\varrho_o(y) = \frac{1}{\nu(y)} = \frac{\varrho_b\,\varrho_d}{\varrho_d\,(1-y) + \varrho_b\,y}. \tag{2.5}$$

Directly from Eq. (2.5) we get the molar volume of oleic phase:

$$\nu(y) = \nu_b\,(1-y) + \nu_d\,y = \frac{\varrho_d\,(1-y) + \varrho_b\,y}{\varrho_b\,\varrho_d}. \tag{2.6}$$

Volume conservation is commonly expressed by the state equation:

$$\frac{\varrho_{ob}}{\varrho_b} + \frac{\varrho_{od}}{\varrho_d} = 1,$$

which holds since $\frac{\varrho_{ob}}{\varrho_b} + \frac{\varrho_{od}}{\varrho_d} = \frac{m_B/V_T}{\varrho_b} + \frac{m_D/V_T}{\varrho_d} = \frac{\varrho_b\,V_B/V_T}{\varrho_b} + \frac{\varrho_d\,V_D/V_T}{\varrho_d} = \frac{V_B+V_D}{V_T} = 1$. We may obtain again the Eq. (2.5): $\frac{\varrho_{ob}}{\varrho_b} + \frac{\varrho_{od}}{\varrho_d} = \frac{(1-y)\varrho_o}{\varrho_b} + \frac{y\varrho_o}{\varrho_d} = \frac{(1-y)\varrho_d + y\,\varrho_b}{\varrho_b\,\varrho_d}\,\varrho_o = 1$.

We also define the normalized oleic molar volume:

$$v(y) \equiv \nu(y)/(\varrho_b\,\varrho_d) = \varrho_d\,(1-y) + \varrho_b\,y; \tag{2.7}$$

so $v(y)$ is positive, namely, we have $\varrho_d \leq v(y) \leq \varrho_b$ for $0 \leq y \leq 1$.

From Eqs. (2.1.ii/iii) and (2.5) we get ϱ_{ob} and ϱ_{od} depending only on y and model constants:

$$(i)\ \ \varrho_{od}(y) = y\,\varrho_o(y), \qquad (ii)\ \ \varrho_{ob}(y) = (1-y)\,\varrho_o(y). \tag{2.8}$$

The viscosity of the liquid oil phase is modeled as:

$$\mu_o(y) = \bar{\mu}_b\,(1-y) + \bar{\mu}_d\,y, \tag{2.9}$$

where $\bar{\mu}_D$ and $\bar{\mu}_B$ are the viscosities of the pure hydrocarbons that exist in the oleic phase. We use Eq. (2.9) instead of the quarter-power-law in [24] since for similar μ_b and μ_d the two expressions differ from tiny percentage. We define the viscosity ratio

$$r(y) = \mu_o(y)/\mu_g = \mu_d\, y + \mu_b\,(1-y), \tag{2.10}$$

where $\mu_b = \bar{\mu}_b/\mu_g$ and $\mu_d = \bar{\mu}_d/\mu_g$.

We define the following:

DEFINITION 2.1. We set $\mathsf{y_r} \equiv -(\mu_b+1)/(\mu_d-\mu_b)$, which is negative.

The following hyperbola plays an important role; we will prove that it is a contact curve.

DEFINITION 2.2. Let $\mathcal{E}_k$ be the hyperbola $\{(s,y)\in\mathbb{R}^2 : (r(y)+1)\,s = r(y)\}$. We define the function $\kappa(y) \equiv r(y)/(r(y)+1)$ for $r(y)\neq -1$, that is, for $y \neq \mathsf{y}_r$. For simplicity, we will also use:

$$\mathsf{K}(s,y) = (r(y)+1)\,s - r(y). \tag{2.11}$$

2.1.3. *Restrictions on model parameters.* For brevity, we use δ_{IJ} to represent the difference between two molar concentrations, that is, $\varrho_i - \varrho_j$, $i,j\in\{b,d,g,v\}$. For instance, we have $\delta_{bd} = \varrho_b - \varrho_d$. In a similar fashion we define $\mu_{db} \equiv \mu_d - \mu_b$.

We need the following:

ASSUMPTION 2.3. We assume that:

(a) molar concentrations satisfy $\varrho_v < \varrho_g < \varrho_d < \varrho_b$;
(b) molar concentration ϱ_v also satisfies $\max\{\,\varrho_g\,\delta_{bd}/\varrho_b\ ,\ \varrho_g\,\mu_{db}/\mu_d\,\} < \varrho_v$;
(c) the viscosities satisfy $1 < \mu_b$ and $\mu_b + \mathfrak{U}_1 < \mu_d < \mu_b + \mathfrak{U}_2$; see Eq. (2.14);
(d) the non-degeneracy condition $\mu_b\,\varrho_b \neq \mu_d\,\varrho_d$ holds.

Assumption 2.3(a) is physically natural; note that $\varrho_d < \varrho_b$ while the mass density usually satisfies the reverse relationship.

DEFINITION 2.4. By Assumption 2.3(b) the following quantities are positive:

$$\pi_1 \equiv \varrho_b\,\varrho_v - \varrho_g\,\delta_{bd}, \quad \pi_2 \equiv \mu_d\,\varrho_v - \varrho_g\,\mu_{db}; \tag{2.12}$$

and by Assumption 2.3(d) we have:

$$\pi_3 \equiv \varrho_b\,\mu_b - \varrho_d\,\mu_d \neq 0. \tag{2.13}$$

For the use of π_1, π_2 and π_3 see, for example, the proof of Lemma 4.13. Assumption 2.3(b) leads to $\mathsf{y}_r < y_x(\grave{s},\grave{y})$; see Eq. (4.14) and the following text. In Assumption 2.3(b) the fractions μ_{db}/μ_d and δ_{bd}/ϱ_b are smaller than 1, so it is possible to satisfy simultaneously $\varrho_v < \varrho_g$ and Assumption 2.3(b). Furthermore, the similarity of fluids B and D leads to the less restrictive Assumption 2.3(b).

The parameters in Assumption 2.3(c) are:

$$(i)\ \mathfrak{U}_1 = \frac{\delta_{bd}^2\,\varrho_v\,\varrho_g}{(\varrho_b+\mu_d\,\varrho_d)\,\pi_1\,\varrho_d}, \quad (ii)\ \mathfrak{U}_2 = \frac{\varrho_v\,\varrho_d\,(\varrho_v+\varrho_b\,\mu_b)}{\varrho_g(\varrho_d\,\varrho_b\,\mu_b+\varrho_d\,\varrho_b+\varrho_v\,\delta_{bd})}\,\mu_b. \tag{2.14}$$

The peculiar constants $\mathfrak{U}_1$ and $\mathfrak{U}_2$ ensure that certain quantities are positive (see Lemmas 4.13 and 4.14). We find $\mu_b + \mathfrak{U}_1 < \mu_d$ is easy to satisfy, we just require that μ_d must be slightly greater than μ_b. On the other hand, the assumption $\mu_d < \mu_b + \mathfrak{U}_2$ is too restrictive; actually, we may have μ_d much greater than required without failure of the desired property in Lemma 4.14.

For simplicity, we introduce the notation; see Eq. (2.3.i):

$$g(y) = \varrho_{ga}(y), \tag{2.15}$$

so we have $\varrho_v \le g(y) \le \varrho_g$ for $0 \le y \le 1$ and $g(y)$ is positive.

2.2. *Molar balance equations for the flow.* We use the porous media notation employed in the literature s_i and f_i for saturation and fractional flow of each phase; again, the subscript o stands for *oleic* and g for *gaseous*. The usual normalization holds:

$$s_o + s_g = 1\,, \quad f_o + f_g = 1, \tag{2.16}$$

where the fractional flow functions f_o and f_g depend on viscosities $\mu_o(y)$ and μ_g and on relative permeabilities, k_o and k_g, indeed:

$$f_o = \big(k_o/\mu_o\big)/\big(k_o/\mu_o + k_g/\mu_g\big)\,, \quad f_g = \big(k_g/\mu_g\big)/\big(k_o/\mu_o + k_g/\mu_g\big). \tag{2.17}$$

Assuming quadratic relative permeabilities and introducing the viscosity ratio $r(y)$, from Eq. (2.10) we obtain:

$$f_o(s_o, y) = \frac{s_o^2}{s_o^2 + r(y)\,(1-s_o)^2}\,, \quad f_g(s_o, y) = 1 - f_o(s_o, y) = \frac{r(y)\,(1-s_o)^2}{s_o^2 + r(y)\,(1-s_o)^2}. \tag{2.18}$$

The molar balance of components A and B in the gaseous phase as well as the molar balance of components B and D in the liquid phase are given by the following equations:

$$\text{gas:} \quad (i)\ \tfrac{\partial}{\partial t}(\varphi \varrho_{ga} s_g) + \tfrac{\partial}{\partial x}(\varrho_{ga} u_g) = 0 \qquad (ii)\ \tfrac{\partial}{\partial t}(\varphi \varrho_{gb} s_g) + \tfrac{\partial}{\partial x}(\varrho_{gb} u_g) = q_b \tag{2.19a}$$

$$\text{oil:} \quad (i)\ \tfrac{\partial}{\partial t}(\varphi \varrho_{ob} s_o) + \tfrac{\partial}{\partial x}(\varrho_{ob} u_o) = -q_b \quad (ii)\ \tfrac{\partial}{\partial t}(\varphi \varrho_{od} s_o) + \tfrac{\partial}{\partial x}(\varrho_{od} u_o) = 0 \tag{2.19b}$$

where the source term q_b represents the mole rate of transfer of oil b from the oleic to the gaseous phase per unit volume and time; it has very large coefficients. For one dimensional flow, Darcy's law is $u = -k\,\partial p/\partial x$; we assumed that pressure is the same in both phases, *i.e.*, we neglect the capillary pressure effect. In (2.19), u_o and u_g are the Darcy velocities of the oleic and gaseous phases. Defining the total Darcy's velocity $u = u_o + u_g$, one can show that $u_o = f_o\, u$ and $u_g = f_g\, u$. Using these expressions for u_o and u_g, adding (2.19a.ii) and (2.19b.i), we obtain conservation equations for the components A, B, and D:

$$\varphi \tfrac{\partial}{\partial t}(\varrho_{ga}\, s_g) + \tfrac{\partial}{\partial x}(u\, \varrho_{ga}\, f_g) = 0, \tag{2.20a}$$

$$\varphi \tfrac{\partial}{\partial t}(\varrho_{gb}\, s_g + \varrho_{ob}\, s_o) + \tfrac{\partial}{\partial x}(u\, \varrho_{gb}\, f_g + u\, \varrho_{ob}\, f_o) = 0, \tag{2.20b}$$

$$\varphi \tfrac{\partial}{\partial t}(\varrho_{od}\, s_o) + \tfrac{\partial}{\partial x}(u\, \varrho_{od}\, f_o) = 0. \tag{2.20c}$$

Gibbs' phase rule, $F = C - P + 2$, for three components ($C = 3$) and two phases ($P = 2$) leads to three degrees of freedom ($F = 2$). Two of these are temperature and pressure, which are assumed to be constant, while the molar fraction y of component D may vary, it is indeed the independent variable. We set the non-thermodynamical variables as follows: oil saturation s_o, and total Darcy velocity u. For simplicity we

write:

$$\begin{aligned} s &\equiv s_o, & f(s,y) &\equiv f_o(s_o,y), \\ &= s^2/D(s,y), & D = D(s,y) &= s^2 + r(y)\,(1-s)^2, \\ \bar f(s,y) &= 1 - f(s,y), & \bar s &= 1-s, \quad \bar y = 1-y. \end{aligned} \tag{2.21}$$

We also have $D = \mathsf{K}\, s + r\,\bar s = s - \mathsf{K}\,\bar s$. Then, system (2.20) may be rewritten as:

$$\varphi\,\tfrac{\partial}{\partial t}\,G(s,y) + \tfrac{\partial}{\partial x}\big(u\,F(s,y)\big) = 0, \text{ where} \tag{2.22}$$

$$G(s,y) = \begin{bmatrix} \varrho_{ga}(y)\,\bar s \\ \varrho_{gb}(y)\,\bar s + \varrho_{ob}(y)\,s \\ \varrho_{od}(y)\,s \end{bmatrix}, \quad F(s,y) = \begin{bmatrix} \varrho_{ga}(y)\,\bar f(s,y) \\ \varrho_{gb}(y)\,\bar f(s,y) + \varrho_{ob}(y)\,f(s,y) \\ \varrho_{od}(y) f(s,y) \end{bmatrix}. \tag{2.23}$$

Here ϱ_{ga} and ϱ_{gb} are known affine functions of y; see Eq. (2.3); ϱ_{ob} and ϱ_{od} are known rational fractions of y; see Eqs. (2.8) and (2.5); f is a rational fraction of s and y; see Eqs. (2.18) and (2.10).

Definition 2.5. By ignoring the seepage velocity u, we define the "reduced" physical domain as $\mathcal{D} = \{(s,y) \in [0,1] \times [0,1]\}$.

3. Characteristic analysis. Equation (2.22) has non-trivial accumulation, therefore the characteristic analysis leads to the generalized eigenvalue problem with matrix:

$DF - \lambda\, DG \equiv J$

$$= \begin{bmatrix} -\varrho_{ga}\,(u\partial_s f - \lambda\,\varphi) & \big(u\bar f - \lambda\varphi\bar s\big)\,\partial_y \varrho_{ga} - u\varrho_{ga}\partial_y f & \varrho_{ga}\bar f \\ \Delta\,(u\partial_s f - \lambda\varphi) & (u-\lambda\varphi)\,\partial_y\varrho_{gb} + (uf - \lambda\,\varphi\, s)\,\partial_y\Delta + u\Delta\partial_y f & \varrho_{gb} + \Delta f \\ \varrho_{od}\,(u\partial_s f - \lambda\,\varphi) & (uf - \lambda\,\varphi\, s)\,\partial_y\varrho_{od} + u\varrho_{od}\partial_y f & \varrho_{od} f \end{bmatrix}, \tag{3.1}$$

where $\Delta = \varrho_{ob} - \varrho_{gb}$. The expression $\det(J)$ is a quadratic polynomial in λ since G does not depend on u. Therefore, J has only two eigenvalues counting multiplicity. We labeled the eigenvalues (characteristic speeds) and eigenvectors with an s meaning *saturation* and with an e meaning *evaporation*.

Lemma 3.1. The generalized characteristic values for Eq. (2.22) are:

$$(i)\ \lambda_s(s,y,u) = \frac{u}{\varphi}\,\partial_s f(s,y), \quad \text{and} \quad (ii)\ \lambda_e(s,y,u) = \frac{u}{\varphi}\,\frac{f(s,y) - \Omega(y)}{s - \Omega(y)}, \text{ where} \tag{3.2}$$

$$(i)\ \Omega(y) = \varrho_v\,\varrho_g\,y\,v(y)/\bar\Omega(y), \quad \text{and} \quad (ii)\ \bar\Omega(y) = \varrho_v\,\varrho_g\,y\,v(y) - \varrho_b\,\varrho_d\,g(y). \tag{3.3}$$

The corresponding right eigenvectors are multiples of

$$\vec r_s(s,y,u) = (1\,,\,0\,,\,0)^T, \tag{3.4a}$$

$$\begin{aligned} \vec r_e(s,y,u) &= (r_e^s, r_e^y, r_e^u)^T = \\ &= \Big((\hat\lambda_e - 1)(\omega_s + \omega_u\, f) - \partial_y f\ ,\ \hat\lambda_s - \hat\lambda_e\ ,\ u\,\omega_u(\hat\lambda_e - 1)(\lambda_s - \lambda_e)\Big)^T, \end{aligned} \tag{3.4b}$$

where

$$(i)\ \hat{\lambda}_s = \partial_s f(s,y), \qquad (ii)\ \hat{\lambda}_e = \frac{f(s,y)-\Omega(y)}{s-\Omega(y)} = \frac{f(s,y)-s}{s-\Omega(y)} + 1 \tag{3.5a}$$

$$(i)\ \omega_s(y) = \varrho_v\,\varrho_g\,\varrho_d/\bar{\Omega}(y), \qquad (ii)\ \omega_u(y) = \varrho_v\,\varrho_d\,\delta_{bg}/\bar{\Omega}(y). \tag{3.5b}$$

The left eigenvector associated to λ_e is

$$l_e = [\,\varrho_{gb}\,\varrho_{od}\,,\ -\varrho_{ga}\,\varrho_{od}\,,\ \varrho_{ga}\,\varrho_{od}\,]\,. \tag{3.6}$$

PROOF OF LEMMA 3.1. We split the second column of J into two terms in order to define two matrices, $\mathcal{J}$ and N; see Eq. (3.1):

$$\mathcal{J} = \begin{bmatrix} -\varrho_{ga}\,(u\partial_s f - \lambda\,\varphi) & \left(u\bar{f} - \lambda\varphi\bar{s}\right)\partial_y\varrho_{ga} & \varrho_{ga}\bar{f} \\ \Delta\,(u\partial_s f - \lambda\varphi) & (u-\lambda\varphi)\,\partial_y\varrho_{gb} + (uf - \lambda\,\varphi\,s)\,\partial_y\Delta & \varrho_{gb} + \Delta f \\ \varrho_{od}\,(u\partial_s f - \lambda\,\varphi) & (uf - \lambda\,\varphi\,s)\,\partial_y\varrho_{od} & \varrho_{od} f \end{bmatrix} \tag{3.7}$$

and

$$N = \begin{bmatrix} -\varrho_{ga}\,(u\partial_s f - \lambda\,\varphi) & -u\varrho_{ga}\partial_y f & \varrho_{ga}\bar{f} \\ \delta_b\,(u\partial_s f - \lambda\varphi) & u\delta_b\partial_y f & \varrho_{gb} + \Delta f \\ \varrho_{od}\,(u\partial_s f - \lambda\,\varphi) & u\varrho_{od}\partial_y f & \varrho_{od} f \end{bmatrix}. \tag{3.8}$$

Then we have $\det(J) = \det(\mathcal{J}) + \det(N)$. Since the first and second columns of N are proportional we have $\det(N) = 0$ and $\det(J) = \det(\mathcal{J})$. In both J and $\mathcal{J}$, the first column is a multiple of $u\partial_s f - \lambda\,\varphi$; so, factoring this term in $\mathcal{J}$ we get $\det(\mathcal{J}) = (u\partial_s f - \lambda\,\varphi)\det(\mathsf{J})$ where

$$\mathsf{J} = \begin{bmatrix} -\varrho_{ga} & \left(u\,\bar{f} - \lambda\,\varphi\,\bar{s}\right)\partial_y\varrho_{ga} & \varrho_{ga}\bar{f} \\ \delta_b & (u-\lambda\varphi)\,\partial_y\varrho_{gb} + (uf - \lambda\,\varphi\,s)\,\partial_y\delta_b & \varrho_{gb} + \delta_b f \\ \varrho_{od} & (uf - \lambda\,\varphi\,s)\,\partial_y\varrho_{od} & \varrho_{od} f \end{bmatrix}. \tag{3.9}$$

Therefore, $\det(J) = 0$ has the trivial solution $\lambda = u\,\partial_s f/\varphi$.

In order to calculate the other eigenvalue, we replace ϱ_{ga} by $g(y)$, see Eq. (2.15), and we rewrite $\varrho_{gb} = \varrho_g - g(y)$, $\partial_y\varrho_{ga} = \varrho_v$, $\partial_y\varrho_{gb} = -\varrho_v$, see Eq. (2.3), $\varrho_{ob} = \varrho_o\bar{y}$ and $\varrho_{od} = \varrho_o y$, see Eq. (2.8), on J and: (i) we subtract the first column multiplied by f from the third one; (ii) we add the first row to the second row; (iii) we add the third column to the first one; then, we get

$$\bar{\mathsf{J}} = \begin{bmatrix} 0 & \left(u\,\bar{f} - \lambda\,\varphi\,\bar{s}\right)\varrho_v & g(y) \\ \bar{y}\,\varrho_o & (u\,f - \lambda\,\varphi\,s)\,\partial_y\varrho_{ob} & \varrho_g \\ y\,\varrho_o & (u\,f - \lambda\,\varphi\,s)\,\partial_y\varrho_{od} & 0 \end{bmatrix}. \tag{3.10}$$

We have $\det(\mathsf{J}) = \det(\bar{\mathsf{J}})$. From

$$\varrho_o = \frac{\varrho_b\,\varrho_d}{g(y)}, \quad \partial_y\varrho_o = \frac{\varrho_b\,\varrho_d\,\delta_{bd}}{g(y)^2}, \quad \partial_y\varrho_{ob} = \varrho_o + y\,\partial_y\varrho_o, \quad \partial_y\varrho_{od} = -\varrho_o + \bar{y}\,\partial_y\varrho_o, \tag{3.11}$$

and $\det(\bar{\mathsf{J}}) = 0$ we obtain λ_e in Eq. (3.2.ii).

The eigenvectors may be checked by computing $J\,\vec{r}_s$, $J\,\vec{r}_e$, and $l_e\,J$. □

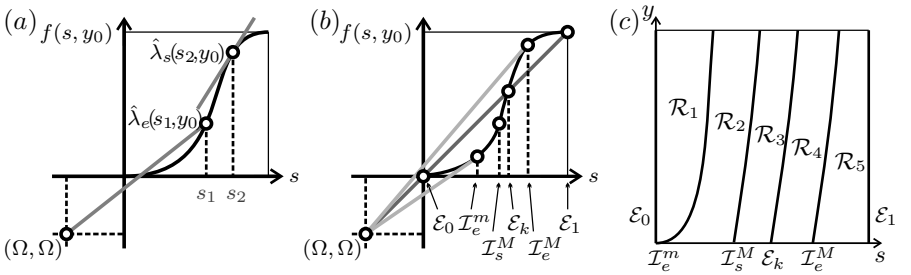

FIG. 1. Consider a fixed y_0. (*a*) The eigenvalue $\hat\lambda_s$ is the slope of a line tangent to the graph of f; the eigenvalue $\hat\lambda_e$ is the slope of the gray chord from $\big(\Omega(y_0),\Omega(y_0)\big)$ to $\big(s,f(s,y_0)\big)$. (*b*) The coincidence locus, $\mathcal{C}=\mathcal{I}_e^m\cup\mathcal{I}_e^M$; the inflection $\mathcal{I}_s^M$, and the curves $\mathcal{E}_0$, $\mathcal{E}_k$, and $\mathcal{E}_1$. (*c*) L-Regions and relative positions on the domain $\mathcal{D}$ of coincidence locus $\mathcal{C}$, inflection $\mathcal{I}_s^M$, and inflection $\mathcal{I}_e=\mathcal{I}_e^m\cup\mathcal{I}_e^M\cup\mathcal{E}_0\cup\mathcal{E}_k\cup\mathcal{E}_1$.

Since the first two coordinates both of $\vec r_s$ and of $\vec r_e$, see Eq. (3.4), do not depend on u, we define the reduced eigenvectors (see ω_s and ω_u in Eq. (3.5b)):

$$\hat{\vec r}_s(s,y)=(1\,,\,0)^T\quad\text{and}\quad\hat{\vec r}_e(s,y)=\big((\hat\lambda_e-1)(\omega_s+\omega_u\,f)-\partial_y f\;,\;\hat\lambda_s-\hat\lambda_e\big).\tag{3.12}$$

The behavior of Ω, Ω', ω_s and ω_u depend on the sign of $\bar\Omega$; see Eqs. (3.3) and (3.5b).

LEMMA 3.2. The functions $\Omega(y)$, $\Omega'(y)$, $\omega_s(y)$ and $\omega_u(y)$ are negative in the interval $(0,1]$; we also have $\Omega(0)=0$, $\Omega'(0)<0$, $\omega_s(0)<0$ and $\omega_u(0)<0$.

PROOF OF LEMMA 3.2. From Eqs. (3.3) and (2.7), we have:

$$\bar\Omega=\varrho_v\,\varrho_g\,\delta_{bd}\,y^2-\varrho_v\,\varrho_d\,\delta_{bg}\,y-\varrho_b\,\delta_{bd}\,\delta_{gv},$$

which is negative for $0\le y\le 1$ because $\bar\Omega(y)$ is an upward concave parabola in y, $\bar\Omega(0)=-\varrho_b\,\varrho_d\,\delta_{gv}<0$ and $\bar\Omega(1)=-\varrho_b\,\varrho_d\,(\varrho_d-\varrho_v)<0$.

The numerator of Ω is positive for $y>0$ and vanishes for $y=0$; the numerators of ω_s and ω_s are positive constants. The derivative of $\Omega(y)$ is

$$\Omega'(y)=-\varrho_v\varrho_g\varrho_b\varrho_d(\varrho_v\delta_{bd}y^2+2\delta_{bd}\delta_{gv}y+\varrho_d\delta_{gv})\big/\,\bar\Omega^2;\tag{3.13}$$

the numerator of $\Omega'(y)$ is negative since it is a concave downward parabola and it undergoes a maximum at $-\delta_{gv}/\varrho_v$ with value $-\varrho_g\,\varrho_b\,\varrho_d\,\delta_{gv}\,\pi_1<0$; see Definition 2.4. □

The reduced eigenvalues, see Eq. (3.5a), have a simple geometrical interpretation; see Fig. 1a. The eigenvalue $\hat\lambda_s$ is the slope of $f(s,y)$ for fixed y. The eigenvalue $\hat\lambda_e$ is the slope of the chord from $(\Omega(y),\Omega(y))$ to $(s,f(s,y))$.

Before studying the coincidence locus, we present four functions that play an important role in our work. We recall Eqs. (2.7), (2.10), (2.15), and (2.11) as well as $\bar s=1-s$. We define:

$$(i)\;\alpha(s,y)=\varrho_v\,\varrho_g\,\bar s^2\,r(y)\,v(y),\qquad(ii)\;\beta(s,y)=\varrho_v\,\varrho_g\,s\,\bar s\,y\,\mathsf{K}(s,y),\tag{3.14a}$$

$$(i)\;\gamma(s)=\varrho_b\,\varrho_d\,s^2,\qquad(ii)\;\eta(s,y)=\varrho_b\,\varrho_d\,s\,\bar s\,g(y)\,\mathsf{K}(s,y),\tag{3.14b}$$

as well as $\grave{\alpha} = \alpha(\grave{s}, \grave{y})$, $\grave{\beta} = \beta(\grave{s}, \grave{y})$, $\grave{\gamma} = \gamma(\grave{s}, \grave{y})$ and $\grave{\eta} = \eta(\grave{s}, \grave{y})$. In order to simplify some expressions we define the following linear combinations of $\grave{\alpha}$ and $\grave{\gamma}$; see Eq. (2.12):

$$(i)\ \grave{\chi} \equiv \grave{\alpha} + \varrho_v\, \grave{\gamma} > 0, \quad (ii)\ \grave{\Pi} \equiv \varrho_d\, \grave{\alpha} + \pi_1\, \grave{\gamma} > 0, \quad (iii)\ \grave{\Phi} \equiv \mu_b\, \grave{\alpha} + \pi_2\, \grave{\gamma} > 0. \tag{3.15}$$

3.1. *The coincidence locus and the inflection locus.* The coincidence locus $\mathcal{C}$ is the set of states (s, y, u) on which the eigenvalues $\lambda_s(s, y, u)$ and $\lambda_e(s, y, u)$ are equal; see Eq. (3.2); alternatively, the projected coincidence locus is the set (s, y) on which the eigenvalues $\hat{\lambda}_s(s, y)$ and $\hat{\lambda}_e(s, y)$ are equal.

On a rarefaction curve, the corresponding eigenvalue must be monotonic, therefore the rarefactions may start and end at the locus defined below.

DEFINITION 3.3. The *i-inflection locus* $\mathcal{I}_i$ is $\{W \in \mathbb{R}^3 : \nabla\lambda_i(W) \cdot r_i(W) = 0\}$.

Lemma 3.4 leads to an explicit expression for $\mathcal{C}$.

LEMMA 3.4. The coincidence locus $\mathcal{C}$ is the zero level of, see Eqs. (2.10), (2.15), and (3.14):

$$C(s, y) = y\, \alpha(s, y)\, \big((r(y) + 1)\, \bar{s}^2 - 1\big) + g(y)\, \gamma(s)\, \big((r(y) + 1)\, s^2 - r(y)\big); \tag{3.16}$$

for each fixed $0 < y < 1$ the function $C(s, y)$ vanishes twice for $0 < s < 1$.

PROOF OF LEMMA 3.4. We have $f(s, y) = s^2/D$ and $\partial_s f(s, y) = 2\, s\, \bar{s}\, r(y)/D^2$ so

$$\lambda_s = \lambda_e \text{ iff } \partial_s f = (f - \Omega)/(s - \Omega) \Leftrightarrow 2\, s\, \bar{s}\, r(y)\, (s - \Omega) = s^2\, D - \Omega\, D^2; \tag{3.17}$$

taking $V = \varrho_v\, \varrho_g\, y\, v(y)$ and $U = \varrho_b\, \varrho_d\, g(y)$ we have $\Omega = V/(V - U)$ and

$$\lambda_s = \lambda_e \Leftrightarrow 2\, s\, \bar{s}\, r(y)\, (s\, (V - U) - V) = s^2\, D\, (V - U) - V\, D^2; \tag{3.18}$$

recalling that $D = s^2 + r(y)\, \bar{s}^2$ we get

$$r(y)\, \bar{s}\, \big(r(y)\, \bar{s}^3 + s^2\, \bar{s} + 2\, s^2 - 2\, s\big)\, V - s^2 \big(s^2 - 2\, \bar{s}\, r(y) + r(y)\, \bar{s}^2\big)\, U = 0. \tag{3.19}$$

Noting that $r(y)\, \bar{s}^3 + s^2\, \bar{s} + 2\, s^2 - 2\, s$ equals $\bar{s}\, ((r(y)+1)\, \bar{s}^2 - 1)$ and that $s^2 - 2\, \bar{s}\, r(y) + r(y)\, \bar{s}^2$ equals $(r(y) + 1)\, s^2 - r(y)$ we obtain Eq. (3.16).

We have: (i) $\gamma(0) = 0$ so $C(0, y) = y\, \alpha(0, y)\, ((r(y) + 1) - 1) = \varrho_v\, \varrho_d\, y\, r(y)^2\, v(y) > 0$, for $y > 0$; (ii) $\alpha(1, y) = 0$ so $C(1, y) = g(y)\, \gamma(1)\, ((r(y) + 1) - r(y)) = \varrho_v\, \varrho_g\, g(y) > 0$; (iii) evaluating C for $(r(y)+1)\, \bar{s}^2 - 1 = 0$ we get $C(s, y) = -2\, g(y)\, \gamma(s) \big((r(y)+1)\, s + r(y)\big) < 0$, so, C has at least two roots for $s \in [0, 1]$. We prove that there are exactly two roots using a geometrical argument based on Fig. 1.b. □

The point $(s, y) = (0, 0)$ is the trivial root of Eq. (3.16), though λ_e is not defined there. This root exists because in (3.17) we multiply both terms by $s - \Omega(y)$ which vanishes at $(0, 0)$. We call $y = \zeta(s)$ the natural continuation of this root; see curve $\mathcal{I}_e^m$ in Fig. 1.c. By the implicit function theorem, this coincidence branch satisfies:

$$\partial_s \zeta(0) = -\left.\frac{\partial_s C}{\partial_y C}\right|_{(0,0)} = 0, \qquad \partial^2_{ss} \zeta(0) = -\left.\frac{\partial^2_{ss} C}{\partial_y C}\right|_{(0,0)} > 0; \quad \text{since}$$

$$\partial_s C(0, 0) = 0, \quad \partial_y C(0, 0) = \mu_b^2\, \varrho_d\, \varrho_v\, \varrho_g > 0, \quad \partial^2_{ss} C(0, 0) = -2\, \varrho_b\, \varrho_d\, \mu_b\, \delta_{gv} < 0.$$

In this work, we also call *inflection* the projection of the *3-D Inflection* on the plane (s, y).

LEMMA 3.5. The inflection locus $\mathcal{I}_s$ associated to λ_s is given by the zero level of

$$\mathcal{I}_s(s,y) = r(y) - 3\,(r(y)+1)\,s^2 + 2\,(r(y)+1)\,s^3; \tag{3.20}$$

this inflection corresponds to a maximum of λ_s, that is, $\mathcal{I}_s \equiv \mathcal{I}_s^M$.

PROOF OF LEMMA 3.5. Since $\vec{r}_s = (1,0,0)$, see Eq. (3.4a), the inflection $\nabla\lambda_s \cdot \vec{r}_s = 0$ is given by $\partial^2_{ss} f = 0$, Eq. (3.2.*i*). Straightforward calculations lead to

$$\partial^2_{ss} f = 2\,r(y)\big(r(y) - 3(r(y)+1)s^2 + 2(r(y)+1)s^3\big)/D^3. \tag{3.21}$$

The ratios $r(y)$ and D are positive, so (3.20) holds. For constant y, Eq. (3.20) has one and only one solution for $s \in [0,1]$ because: (i) $\mathcal{I}_s(0,y) = r(y) > 0$; (ii) $\mathcal{I}_s(1,y) = -1$; (iii) and $\mathcal{I}_s(s,y_0)$ is monotonically decreasing for $s \in [0,1]$ and fixed y_0, $\partial_s \mathcal{I}_s(s,y) = -6\,s\,\bar{s}\,(r(y)+1) \le 0$. Therefore, the dot product $\nabla\lambda_s \cdot \vec{r}_s$ is positive on the left hand side of $\mathcal{I}_s$ and negative on the right hand side of $\mathcal{I}_s$, leading to a maximum of λ_s on the integral curve. □

We need the hyperbola $\mathcal{E}_k$; see Definition 2.2, and the following sets:

DEFINITION 3.6. We define:

$$\mathcal{E} \equiv \{(s,y) \in \mathbb{R}^2 : s = f(s,y)\},\ \mathcal{E}_0 \equiv \{(s,y) \in \mathbb{R}^2 : s = 0\},$$

and

$$\mathcal{E}_1 \equiv \{(s,y) \in \mathbb{R}^2 : s = 1\}.$$

LEMMA 3.7. The projection of $\mathcal{I}_i$ coincides with $\nabla\hat{\lambda}_i(s,y) \cdot \hat{\vec{r}}_i(s,y) = 0$, $i \in \{s,e\}$.

Proof. For saturation inflection the lemma holds since the third coordinate of $\vec{r}_s$ vanishes; see Eq. (3.4a). For evaporation inflection we have:

$$\nabla\hat{\lambda}_e \hat{\vec{r}}_e = \frac{u}{\varphi(s-\Omega)}\,(\hat{\lambda}_s - \hat{\lambda}_e)\,(\hat{\lambda}_e - 1)\,\big(\omega_s + \omega_u\,f + \Omega'\big),$$

which differs from (3.22c). However, since $\omega_s + \omega_u\,f + \Omega'$ and $\omega_s + \omega_u\,f + \Omega' + \omega_u\,(f-\Omega)$ are negative the lemma holds. □

LEMMA 3.8. Consider constant u and a family of states $\big(s(t), y(t)\big)$ which belongs to $\mathcal{E}$. The curve $\big(s(t), y(t), u\big)$ is a contact associated to λ_e, *i.e.*, it is: (i) a contour line of λ_e; (ii) an inflection locus associated to λ_e; (iii) an integral curve of r_e.

PROOF OF LEMMA 3.8. (i) From Eq. (3.2.ii) we have $f(s,y) = s$ iff $\hat{\lambda}_e = 1$ iff $\lambda_e = u/\varphi$; (ii) that was proved in Lemma 3.10; (iii) from the condition $f(s,y) - s = 0$ and from the fact that u is constant on the curve we know that the curve velocity $(\dot{s}, \dot{y}, \dot{u})$ satisfies $\mathrm{d}/\mathrm{d}t(f(s,y) - s) = \partial_s f\,\dot{s} + \partial_y f\,\dot{y} - \dot{s} = 0$ and $\dot{u} = 0$. So, vector $(\dot{s}, \dot{y}, \dot{u})$ is a multiple of $(\partial_y f, 1 - \partial_s f, 0)$. The eigenvector r_e for $\hat{\lambda}_e = 1$ becomes $(\partial_y f, 1 - \hat{\lambda}_s, 0)$, that is, also a multiple of $(\dot{s}, \dot{y}, \dot{u})$, so (iii) holds. □

We have $\mathcal{E} = \mathcal{E}_0 \cup \mathcal{E}_k \cup \mathcal{E}_1$, since $s = f(s,y) \Leftrightarrow s\,D = s^2$ iff $s\,(D - s) = 0$ iff $s\,\mathsf{K}\,\bar{s} = 0$.

LEMMA 3.9. The curve $\mathcal{E}_k$ lies on the right of $\mathcal{I}_s^M$.

PROOF OF LEMMA 3.9. Taking $s = \kappa(y)$ in Eq. (3.20) we get $\mathcal{I}(\kappa(y), y)$ equal to $-\kappa(y)(r(y) - 1)/(r(y) + 1) < 0$; the ratio $r(y)$ has a minimum value μ_b which is greater

than 1 by Assumption 2.3(c). Therefore, $\mathcal{E}_k$ lies on the negative side of $\mathcal{I}_s(s,y)$; see Eq. (3.20), that is, on the right of $\mathcal{I}_s^M$. □

Usually, perpendicular vectors have non-perpendicular projections. However, in this model, the inflection is also the set where the projected vectors are perpendicular: $\nabla\hat{\lambda}_i(s,y)\cdot\hat{\vec{r}}_i(s,y)=0$, $i\in\{s,e\}$; see Eq. (3.12) and Lemma 3.7. We denote the inflection as $\mathcal{I}_i^M$ and $\mathcal{I}_i^m$ wherever the value of λ_i reaches a maximum or minimum along the integral curves, respectively.

We obtain an explicit expression for the saturation inflection; see Lemma 3.5. The inflection locus $\mathcal{I}_e$ is the union $\mathcal{C}\cup\mathcal{E}$; see Lemma 3.10.

LEMMA 3.10. The inflection locus $\mathcal{I}_e$ associated to λ_e is the union $\mathcal{C}\cup\mathcal{E}$.

PROOF OF LEMMA 3.10. From Eqs. (3.2.ii), and (3.4) we have:

$$\nabla\lambda_e=\frac{1}{\varphi(s-\Omega)}\big(u\,(\hat{\lambda}_s-\hat{\lambda}_e)\,,\,u\,\partial_y f+u\,(\hat{\lambda}_e-1)\,\Omega'\,,\,f-\Omega\big);\tag{3.22a}$$

$$\vec{r}_e=\Big[\,(\hat{\lambda}_e-1)\,(\omega_s+\omega_u\,f)-\partial_y f\,,\,\hat{\lambda}_s-\hat{\lambda}_e\,,\,u\,(\hat{\lambda}_e-1)\,\omega_u\,(\hat{\lambda}_s-\hat{\lambda}_e)\,\Big]^T;\tag{3.22b}$$

$$\nabla\lambda_e\cdot\vec{r}_e=\frac{u}{\varphi(s-\Omega)}\,(\hat{\lambda}_s-\hat{\lambda}_e)\,(\hat{\lambda}_e-1)\,\big(\omega_s+\omega_u\,f+\Omega'+\omega_u\,(f-\Omega)\big).\tag{3.22c}$$

Therefore, $\nabla\lambda_e\cdot\vec{r}_e=0$ if: (i) $\hat{\lambda}_s-\hat{\lambda}_e=0$, that is, at coincidence locus; or (ii) $\hat{\lambda}_e-1=0$, that is, if $f=s$ which defines $\mathcal{E}$; see Eq. (3.5a.ii).

The factors ω_s, $\omega_u\,f$, Ω', and $\omega_u\,(f-\Omega)$ are negative; see Lemma 3.2. □

The coincidence is $\mathcal{C}=\mathcal{I}_e^m\cup\mathcal{I}_e^M$. The three parts of $\mathcal{E}$ ($\mathcal{E}_0$, $\mathcal{E}_k$, and $\mathcal{E}_1$) are contact curves associated to λ_e; see lemma 3.8.

3.2. *L-regions.* In this section we define *L-regions* in the usual sense; see, for instance, [15]. First, we need to know the relative location of the codimension-1 loci.

For $(s,y)\in\mathcal{C}$ we have $\hat{\vec{r}}_s(s,y)\equiv\hat{\vec{r}}_e(s,y)=(1,0)$, so it is possible to use Fig. 1.b (where y is constant) to see that $\hat{\lambda}_e$ has a minimum through the integral curve of $\hat{\vec{r}}_e$ on left coincidence, marked as $\mathcal{I}_e^m$ in Fig. 1.b, and a maximum for right coincidence, marked as $\mathcal{I}_e^M$. The "S" shape of f ensures that: (i) the curves appear, from the left to the right, in this order: $\mathcal{E}_0$, $\mathcal{I}_e^m$, $\mathcal{I}_s^M$, $\mathcal{I}_e^M$, $\mathcal{E}_1$; (ii) $\mathcal{E}_k$ lies between $\mathcal{I}_e^m$ and $\mathcal{I}_e^M$. Lemma 3.9 states that curve $\mathcal{E}_k$ lies on the right of $\mathcal{I}_s^M$. See Figs. 1.b and 1.c for the locations of $\mathcal{E}_0$, $\mathcal{I}_e^m$, $\mathcal{I}_s^M$, $\mathcal{E}_k$, $\mathcal{I}_e^M$, and $\mathcal{E}_1$.

DEFINITION 3.11. We define the following L-regions: $\mathcal{R}_1$ between $\mathcal{E}_0$ and $\mathcal{I}_e^m$; $\mathcal{R}_2$ between $\mathcal{I}_e^m$ and $\mathcal{I}_s^M$; $\mathcal{R}_3$ between $\mathcal{I}_s^M$ and $\mathcal{E}_k$; $\mathcal{R}_4$ between $\mathcal{E}_k$ and $\mathcal{I}_e^M$; $\mathcal{R}_5$ between $\mathcal{I}_e^M$ and $\mathcal{E}_1$. We set also $\mathcal{R}_L=\mathcal{R}_1\cup\mathcal{R}_2\cup\mathcal{R}_3$ and $\mathcal{R}_R=\mathcal{R}_4\cup\mathcal{R}_5$, the regions on the left and on the right side of curve $\mathcal{E}_k$, respectively.

We remark that evaporation rarefactions cross neither $\mathcal{E}_0$, $\mathcal{E}_k$, nor $\mathcal{E}_1$; therefore, $\mathcal{R}_L$ and $\mathcal{R}_R$ are disjoint regions as far as the evaporation rarefaction foliation is concerned; see Fig. 7.b.

For $(s,y)\in\mathcal{R}_R$ we have:

$$0<\bar{s}<\tfrac{1}{\mu_d+1},\quad 0<\eta<\tfrac{\varrho_b\,\varrho_d\,\varrho_g}{4}\,\tfrac{1}{\mu_b+1},\quad \varrho_v\varrho_d\,\tfrac{\mu_b\,(\varrho_b\,\mu_b+\varrho_g)}{(\mu_b+1)^2}\le\alpha+\varrho_v\,\gamma.\tag{3.23}$$

3.3. *Reduced rarefaction curves.* From the sign of $\mathcal{C}$, see Eq. (3.16), we know that in L-regions $\mathcal{R}_1$ and $\mathcal{R}_5$ the inequality $\hat{\lambda}_s<\hat{\lambda}_e$ holds (that is, $\hat{\lambda}_s=\lambda_1$ is the slowest

TABLE 1. Direction of the evaporation integral curve and direction of rarefaction speed growth.

Sector	$\mathcal{E}_0$	$\mathcal{R}_1$	$\mathcal{I}_e^m$	$\mathcal{R}_{2/3}$	$\mathcal{E}_k$	$\mathcal{R}_4$	$\mathcal{R}_4$	$\mathcal{R}_4$	$\mathcal{I}_e^M$	$\mathcal{R}_5$	$\mathcal{E}_1$
Family	-	2	-	1	1	1	1	1	-	2	-
$r_e^y \equiv \hat{\lambda}_s - \hat{\lambda}_e$	$\ominus$	$\ominus$	0	$\oplus$	$\oplus$	$\oplus$	$\oplus$	$\oplus$	0	$\ominus$	$\ominus$
$\hat{\lambda}_e - 1$	0	$\ominus$	$\ominus$	$\ominus$	0	$\oplus$	$\oplus$	$\oplus$	$\oplus$	$\oplus$	0
r_e^s	0	$\oplus$	$\oplus$	$\oplus$	$\oplus$	$\oplus$	0	$\ominus$	$\ominus$	$\ominus$	0
$\nabla\lambda_e \cdot \vec{r}_e$	0	$\ominus$	0	$\oplus$	0	$\ominus$	$\ominus$	$\ominus$	0	$\oplus$	0
Rarefaction	|	$\nwarrow$	—	$\nearrow$	/	$\swarrow$	$\downarrow$	$\searrow$	—	$\swarrow$	|

characteristic and $\hat{\lambda}_e = \lambda_2$ is the fastest); on the other hand, in L-regions $\mathcal{R}_2$, $\mathcal{R}_3$ and $\mathcal{R}_4$ we have $\hat{\lambda}_s > \hat{\lambda}_e$ (that is, $\hat{\lambda}_s = \lambda_1$ and $\hat{\lambda}_e = \lambda_2$).

The rarefactions curves associated to λ_s are horizontal ($\hat{\vec{r}}_s = (1, 0)$) and point to $\mathcal{I}_2^M$; see Fig. 7.b and Lemma 3.5.

The rarefactions associated to λ_e are also represented in Fig. 7.b; they are the curved rarefactions. In order to determine the orientation of the λ_e-rarefaction we need to study both $\hat{\vec{r}}_e$ and $\nabla\lambda_e \cdot \vec{r}_e$. In Table 1 we present the sign of $\hat{\lambda}_s - \hat{\lambda}_e$, $\hat{\lambda}_e - 1$, r_e^s and $\nabla\lambda_e \cdot \vec{r}_e$ in the L-regions. The sign of the first coordinate of $\vec{r}_e$, r_e^s, see Eq. (3.22b), is the most difficult to assess. The factors $\omega_s + \omega_u f$ and $\partial_y f$ are negative, so r_e^s is positive when $\hat{\lambda}_e - 1$ is negative; when $\hat{\lambda}_e - 1$ is null then r_e^s is positive; when $\hat{\lambda}_e - 1$ is positive then r_e^s may be positive or negative due to the positive factor $-\partial_y f$. For $s = 1$, $\hat{\lambda}_e - 1$, $\partial_y f$ vanish as well as r_e^s. The factor $\hat{\lambda}_e - 1$ is linear in $\bar{s}$ while $\partial_y f$ is quadratic in $\bar{s}$, so r_e^s is negative close to $s = 1$. Therefore, r_e^s has a root somewhere between $\mathcal{E}_k$ and $\mathcal{E}_1$. Since $\vec{r}_e$ is vertical when r_e^s vanishes and it is horizontal at $\mathcal{I}_e^M$, the root of r_e^s may lie between $\mathcal{E}_k$ and $\mathcal{I}_e^M$. The orientation of these rarefactions are sketched on the last row of Table 1.

4. The Rankine-Hugoniot locus. Consider a state $\grave{W} = (\grave{s}, \grave{y}, \grave{u})$, usually called a *left state*, such that $(\grave{s}, \grave{y})$ lies in the (reduced) physical domain $\mathcal{D} = [0, 1] \times [0, 1]$ and $\grave{u} > 0$. The Rankine-Hugoniot conditions are (see [23]):

$$H(W, \grave{W}) \equiv uF(W) - \grave{u}F(\grave{W}) - \sigma\big(G(W) - G(\grave{W})\big) = 0 \tag{4.1}$$

and the Rankine Hugoniot locus from $\grave{W}$ is:

$$\mathscr{H}(\grave{W}) = \Big\{W = (s, y, u) : \exists\sigma \in \mathbb{R},\, H(W, \grave{W}) = 0\Big\}. \tag{4.2}$$

Following [10] we rewrite Eq. (4.1) as a linear system in u, $\grave{u}$, and σ (see Eq. (2.23)):

$$M\begin{bmatrix} u \\ \grave{u} \\ \varphi\,\sigma \end{bmatrix} \equiv \begin{bmatrix} \varrho_{ga}\bar{f} & -\grave{\varrho}_{ga}\grave{\bar{f}} & -\varrho_{ga}\bar{s}+\grave{\varrho}_{ga}\grave{\bar{s}} \\ \varrho_{gb}\bar{f}+\varrho_{ob}f & -\grave{\varrho}_{gb}\grave{\bar{f}}-\grave{\varrho}_{ob}\grave{f} & -\varrho_{gb}\bar{s}-\varrho_{ob}s+\grave{\varrho}_{gb}\grave{\bar{s}}+\grave{\varrho}_{ob}\grave{s} \\ \varrho_{od}f & -\grave{\varrho}_{od}\grave{f} & -\varrho_{od}s+\grave{\varrho}_{od}\grave{s} \end{bmatrix}\begin{bmatrix} u \\ \grave{u} \\ \varphi\sigma \end{bmatrix}=0, \tag{4.3}$$

where $\bar{s} = 1 - s$, $\grave{s} = 1 - s$, $\grave{\bar{s}} = 1 - \grave{s}$, $f = f(s, y)$, $\bar{f} = 1 - f$, $\grave{f} = f(\grave{s}, \grave{y})$, $\grave{\bar{f}} = 1 - \grave{f}$, $\varrho_{ij} = \varrho_{ij}(y)$ and $\grave{\varrho}_{ij} = \varrho_{ij}(\grave{y})$ with $ij \in \{ga, gb, ob, od\}$.

The Hugoniot locus is the solution set of Eq. (4.3) eliminating σ. The trivial solution $(u, \grave{u}, \varphi\,\sigma) = (0, 0, 0)$ of Eq. (4.3) does not belong to the Hugoniot locus since we require $\grave{u} > 0$. From Eq. (4.3) we obtain u and σ as functions of $(s, y, \grave{s}, \grave{y}, \grave{u})$. On the Hugoniot locus, $\det(M) = 0$ and Eq. (4.3) hold. The matrix M depends only on s and y, and we define the (projected) Hugoniot locus as the null set of the determinant of M. The determinant of matrix M in Eq. (4.3) is; see Eq. (3.14):

$$\frac{\varrho_b\,\varrho_d\,(y-\grave{y})}{\grave{D}\,\grave{v}\,D\,v(y)}\,\mathcal{Z}(s,y,\grave{s},\grave{y}),\ \text{ where }\ \mathcal{Z}=\frac{\grave{\beta}\,\alpha-\grave{\alpha}\,\beta}{\varrho_v\,\varrho_g}+\frac{\grave{\eta}\,\gamma-\grave{\gamma}\,\eta}{\varrho_b\,\varrho_d}, \tag{4.4}$$

where α, β, γ, and η depend on (s, y) while $\grave{\alpha}$, $\grave{\beta}$, $\grave{\gamma}$, and $\grave{\eta}$ depend on $(\grave{s}, \grave{y})$.

The following holds:

$$g(y)-\grave{g}=\varrho_v\,(y-\grave{y}),\quad D(s,y)-s=\bar{s}\,\mathsf{K}(s,y),\quad D(s,y)-s^2=\bar{s}\,r(y). \tag{4.5}$$

The coefficients of $\mathcal{Z}$ are; see Eq. (4.8):

$$\mathrm{A}(s,\grave{s},\grave{y})=\mu_{db}\,\bar{s}^2\left(\grave{\chi}\,s+\delta_{bd}\,\grave{\beta}\right), \tag{4.6a}$$

$$\mathrm{B}(s,\grave{s},\grave{y})=-\bar{s}\left(\grave{\chi}\,s^2-\left(\mu_b\,\grave{\alpha}+(2\,\mu_b\,\varrho_v-\pi_2)\grave{\gamma}\right)s\,\bar{s}-(\pi_3+2\,\varrho_d\,\mu_{db})\,\grave{\beta}\,\bar{s}\right), \tag{4.6b}$$

$$\mathrm{C}(s,\grave{s},\grave{y})=\delta_{gv}\,\grave{\gamma}\,(\mu_b\,\bar{s}-s)\,s\,\bar{s}+\grave{\eta}\,s^2+\mu_b\,\varrho_d\,\grave{\beta}\,\bar{s}^2, \tag{4.6c}$$

where π_2, π_3, $\grave{\alpha}$, $\grave{\beta}$, $\grave{\gamma}$, $\grave{\eta}$, and $\grave{\chi}$ are given in Eqs. (2.12), (2.13), (3.14), and (3.15.i).

The coefficients of $\mathcal{Z}$ are; see Eq. (4.9):

$$\mathrm{L}(y,\grave{s},\grave{y})=(r(y)+1)\,(\grave{\chi}\,y+\delta_{gv}\grave{\gamma}),\qquad \mathrm{M}(y,\grave{s},\grave{y})=\grave{\eta}-\mathrm{L}(y)-\mathrm{N}(y)-\mathrm{P}(y), \tag{4.7a}$$

$$\mathrm{N}(y,\grave{s},\grave{y})=r(y)\,(\grave{\chi}\,y+\delta_{gv}\grave{\gamma})-2\,\mathrm{P}(y),\quad \mathrm{P}(y,\grave{s},\grave{y})=\grave{\beta}\,v(y)\,r(y). \tag{4.7b}$$

Definition 4.1. The projected Hugoniot locus from $(\grave{s}, \grave{y})$ has two parts, the straight line part given by $y = \grave{y}$, named *saturation Hugoniot*; and the curved part given by: $\{(s, y) \in \mathbb{R}^2 : \mathcal{Z}(s, y, \grave{s}, \grave{y}) = 0\}$, named *evaporation Hugoniot*.

In order to study the behavior of the Hugoniot locus, we restrict the state $(\grave{s}, \grave{y})$ to the physical domain $\mathcal{D}$ but the state (s, y) may lie on the whole $\mathbb{R}^2$.

The function $\mathcal{Z}$ may be written as a quadratic polynomial in y; its coefficients are third order polynomials in s. These polynomials are denoted as A, B and C. They have coefficients depending on $(\grave{s}, \grave{y})$ and on the model parameters except φ. Indeed, straight from Eq. (4.4) we have:

$$\mathcal{Z}(s,y,\grave{s},\grave{y})=\mathrm{A}\,y^2+\mathrm{B}\,y+\mathrm{C}, \tag{4.8}$$

where A, B, and C depend on $(s, \grave{s}, \grave{y})$; see Eq. (4.6).

The function $\mathcal{Z}$ may also be written as a cubic polynomial in s with coefficients that are second order polynomials in y:

$$\mathcal{Z}(s,y,\grave{s},\grave{y})=\mathrm{L}\,s^3+\mathrm{M}\,s^2+\mathrm{N}\,s+\mathrm{P}, \tag{4.9}$$

where L, M, N, and P depend on $(y, \grave{s}, \grave{y})$; see Eq. (4.7).

We remark that the evaporation Hugoniot consists of several *branches*. Equation (4.8) is quadratic in y, therefore the following definitions are natural.

Definition 4.2. The solutions of Eq. (4.8) are $\mathsf{B}_+(s)$ and $\mathsf{B}_-(s)$ as in Appendix A.

Using Eq. (4.6) one sees that the discriminant of Eq. (4.8) is the 6^{th} degree polynomial:

$$\Delta(s;\grave{s},\grave{y}) = (1-s)^2\, Q(s,\grave{s},\grave{y}), \tag{4.10}$$

where $Q(s,\grave{s},\grave{y}) = \sum_{i=0}^{4} X_i\, s^i$ is a polynomial in s with coefficients depending on $(\grave{s},\grave{y})$:

$$X_0 = x_1^2, \quad X_1 = 2\,x_1\big(\grave{\Phi} - x_1\big), \quad X_2 = (\grave{\Phi} - x_1)^2 - 2\,x_1\,z_1 + x_3(x_2 + 2\,\grave{\Phi}), \tag{4.11a}$$

$$X_3 = 2\,x_1\,z_1 - 2\,\grave{\Phi}(x_3 + z_2) - 2\,x_2\,\grave{\chi}, \quad X_4 = z_2^2, \tag{4.11b}$$

where $x_1 = \pi_3\,\grave{\beta}$, $x_2 = 2\,\mu_{db}\,\grave{\eta}$, $x_3 = -2\,\delta_{bd}\,\grave{\beta}$, $z_1 = \grave{\Phi} - \grave{\chi}$, and $z_2 = \grave{\Phi} + \grave{\chi}$; see Eqs. (2.12), (3.14), and (3.15).

See Eq. (4.9); we define the following discriminant where $\mathrm{L}(y,\grave{s},\grave{y}) = 0$:

$$\boldsymbol{\Delta}(y,\grave{s},\grave{y}) = \mathrm{N}^2(y,\grave{s},\grave{y}) - 4\,\mathrm{M}(y,\grave{s},\grave{y})\,\mathrm{P}(y,\grave{s},\grave{y}). \tag{4.12}$$

On the saturation Hugoniot curve, shock speed and seepage velocity are trivial:

Lemma 4.3. The Rankine-Hugoniot condition has the following solution:

$$s \neq \grave{s}, \quad y = \grave{y}, \quad u = \grave{u}, \quad \sigma = \frac{\grave{u}}{\varphi}\,\frac{f(s,\grave{y}) - f(\grave{s},\grave{y})}{s - \grave{s}}. \tag{4.13}$$

Proof of Lemma 4.3. In the Hugoniot condition, see Eq. (4.2), each equation is:

$$u\,F_i(s,y) - \grave{u}\,F_i(\grave{s},\grave{y}) - \varphi\,\sigma\big(G_i(s,y) - G_i(\grave{s},\grave{y})\big) = 0.$$

Taking $y = \grave{y}$ and $u = \grave{u}$ we get: $\sigma = \frac{1}{\varphi}\,\frac{\grave{u}\,F_i(s,\grave{y}) - \grave{u}\,F_i(\grave{s},\grave{y})}{G_i(s,\grave{y}) - G_i(\grave{s},\grave{y})} = \frac{\grave{u}}{\varphi}\,\frac{f(s,\grave{y}) - f(\grave{s},\grave{y})}{s - \grave{s}}$. Since the velocity σ does not depend on i, the lemma holds. □

Lemmas 3.1 and 4.3 state that there exist shocks and rarefactions along which the variables y and u are kept constant. Therefore, the solution of the Riemann problem for $\grave{W} = (\grave{s},\grave{y},\grave{u})$ and $W = (s,\grave{y},\grave{u})$ is obtained from the one dimensional problems studied by Oleinik, see [19], with an extra eigenvalue λ_e. Since the function $f(s,y)$ for fixed y has an "S" shape, then this solution is similar to the Buckley-Leverett's solution, see [2], again with an extra eigenvalue λ_e.

The following lemma presents one of the fundamental features of our problem: persistence of double contacts. Usually, perturbations of the left state leads to the loss of the double contact, since they are codimension-1 structures; see [20, 21]. On the other hand, our problem has open sets of states for which there are double characteristic shocks. This phenomenon leads to solutions without intermediate state for an open set of initial data as shown in Example 5.3 in Section 5.2 as well as in [17, 22].

Lemma 4.4. If the shock from $\grave{W} = (\grave{s},\grave{y},\grave{u})$ to $W = (s,\grave{y},\grave{u})$ is right characteristic, then it is also left characteristic; and vice versa.

Proof of Lemma 4.4. Using the right characteristic shock condition $\lambda_e(s,\grave{y},\grave{u}) = \sigma$ and Eqs. (3.2.ii) and (4.13) we obtain $\lambda_e(s,\grave{y},\grave{u})$ equal to

$$\tfrac{\grave{u}}{\varphi}\,\tfrac{f(s,\grave{y}) - \Omega(\grave{y})}{s - \Omega(\grave{y})} = \tfrac{\grave{u}}{\varphi}\,\tfrac{f(s,\grave{y}) - f(\grave{s},\grave{y})}{s - \grave{s}} = \tfrac{\grave{u}}{\varphi}\,\tfrac{f(s,\grave{y}) - \Omega(\grave{y}) - f(s,\grave{y}) + f(\grave{s},\grave{y})}{s - \Omega(\grave{y}) - s + \grave{s}} = \tfrac{\grave{u}}{\varphi}\,\tfrac{f(\grave{s},\grave{y}) - \Omega(\grave{y})}{\grave{s} - \Omega(\grave{y})} = \lambda_e(\grave{s},\grave{y},\grave{u}).$$

Thus, the shock is also left characteristic; the reciprocal holds by the same argument. □

Possible self-intersections of the Hugoniot locus occur when the implicit function theorem does not assure this locus is locally a curve (for a discussion on bifurcation and self-intersection see [22]). We define this set as *self-intersection Hugoniot locus* as defined below, that is, the set where matrix $[D(uF_i) - \sigma DG_i\,, \grave{G}_i - G_i]$ is not full rank.

DEFINITION 4.5. The self-intersection Hugoniot locus is:

$$\mathcal{B} = \{\grave{W} \in \mathbb{R}^n : \exists W \in \mathscr{H}(\grave{W}) \setminus \grave{W},\ \sigma = \lambda_i(W) \text{ and } l_i(W)\big(G(W) - G(\grave{W})\big) = 0\}.$$

The double characteristic shock occurs at self-intersection of the Hugoniot locus; see the next lemma.

LEMMA 4.6. Let the shock between $\grave{W} = (\grave{s}, \grave{y}, \grave{u})$ and $W = (s, \grave{y}, \grave{u})$ be right characteristic associated to λ_e. Then $\grave{W}$ and W belong to the self-intersection Hugoniot locus.

PROOF OF LEMMA 4.6. By assumption we have $\sigma(\grave{W}, W) = \lambda_e(W)$. In order to prove that W belongs to $\mathcal{B}$ we need to prove that $l_e(\grave{W})\big(G(W) - G(\grave{W})\big) = 0$. From $y = \grave{y}$ we get: $G - \grave{G} = (s - \grave{s})\ [-\grave{\varrho}_{ga}\,,\ \grave{\varrho}_{ob} - \grave{\varrho}_{gb}\,,\ \grave{\varrho}_{od}]^T$. Thus, we have, see Eq. (3.6):

$$l_e(\grave{W})\big(G - \grave{G}\big) = (s - \grave{s})\ [\,\varrho_{gb}\,\varrho_{od}\,,\ -\varrho_{ga}\,\varrho_{od}\,,\ \varrho_{ga}\,\varrho_{od}\,]\,[-\grave{\varrho}_{ga}\,,\ \grave{\varrho}_{ob} - \grave{\varrho}_{gb}\,,\ \grave{\varrho}_{od}]^T = 0.$$

We have also $(s, y, u) \in \mathcal{B}$ since from Lemma 4.4 we have $\sigma(\grave{W}, W) = \lambda_e(\grave{W})$. □

4.1. *The behavior of the evaporation Hugoniot.* In this section our goal is to describe the shape of the evaporation Hugoniot for all possible left states in the physical domain.

We start the study of Hugoniot at special left states for which it is possible to give an explicit expression for the evaporation Hugoniot. We need the following definition, see Eqs. (3.14) and (3.15):

$$\grave{y}_x \equiv y_x(\grave{s}, \grave{y}) \equiv -\delta_{gv}\,\grave{\gamma}\,/\,\grave{\chi}. \tag{4.14}$$

LEMMA 4.7. Consider the states $(\grave{s}, \grave{y}) \in \mathcal{E} \cap \mathcal{D}$. The evaporation Hugoniot for such states consists of $\mathcal{E}$ and the horizontal line $y = y_x(\grave{s}, \grave{y})$, as in Eq. (4.14). (See Figs. 3.*a*/*e*/*i*.)

PROOF OF LEMMA 4.7. Consider $\mathcal{Z}$ of Eq. (4.4):

(i) Taking $\grave{s} = 0$ (see Fig. 3.a.) we get $\grave{\beta} = 0$, $\grave{\gamma} = 0$, $\grave{\eta} = 0$ and then

$$\mathcal{Z}(s, y, \grave{s}, \grave{y}) = \grave{\alpha}\,\beta(s, y)\,/\,(\varrho_v\,\varrho_g) = \varrho_v\,\varrho_g\,\grave{r}\,\grave{v}\,s\,\bar{s}\,y\,\mathsf{K}(s, y).$$

Since $y_x(0, \grave{y}) = 0$ the factor y equals $y - y_x(\grave{s}, \grave{y})$ so the lemma holds for $\grave{s} = 0$. (We remark that $\grave{v}\,\grave{r}$ cancels in the (4.4) without changing the solution.)

(ii) Taking $\grave{s} = \kappa(\grave{y})$ (see Fig. 3.e) we get $\grave{\beta} = 0$, $\grave{\eta} = 0$ and then $\mathcal{Z}$ equals

$$-\tfrac{\beta(s,y)\,\alpha(\kappa(\grave{y}),\grave{y})}{\varrho_v\,\varrho_g} - \tfrac{\gamma(\kappa(\grave{y}))\,\eta(s,y)}{\varrho_b\,\varrho_b} = -s\,\bar{s}\,\mathsf{K}(s, y)\,\tfrac{\grave{r}}{(\grave{r}+1)^2}\big(\varrho_v(\varrho_g\,\grave{v} + \varrho_b\,\varrho_d\,\grave{r})\,y + \varrho_b\,\varrho_d\,\delta_{gv}\,\grave{r}\big).$$

Since $y_x(\kappa(\grave{y}), \grave{y}) = -\varrho_b\,\varrho_d\,\delta_{gv}\,\grave{r}/\varrho_v\,\big(\varrho_g\,\grave{v} + \varrho_b\,\varrho_d\,\grave{r}\big)$, the lemma holds for $(\grave{s}, \grave{y}) \in \mathcal{E}_k$.

(iii) Taking $\grave{s} = 1$ (see Fig. 3.i) we get $\grave{\alpha} = 0$, $\grave{\beta} = 0$, $\gamma(\grave{s}, \grave{y}) = \varrho_b\,\varrho_d$, $\grave{\eta} = 0$ and then

$$\mathcal{Z}(s, y, \grave{s}, \grave{y}) = \eta(s, y) = \varrho_b\,\varrho_d\,s\,\bar{s}\,g(y)\,\mathsf{K}(s, y).$$

Since $y_x(1, \grave{y}) = -\delta_{gv}/\varrho_v$ then $g(y) = \varrho_v\,(y - y_x(\grave{s}, \grave{y}))$ so the lemma holds for $\grave{s} = 1$. □

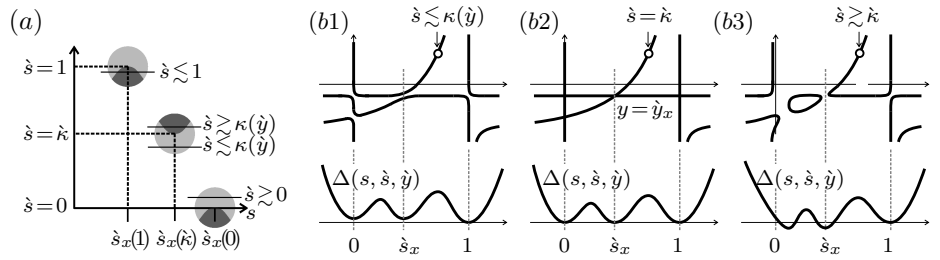

FIG. 2. (*a*) The sign of $\Delta(s,\dot{s},\dot{y})$: positive for light gray shadow; negative for dark gray shadow. (*b*) Evaporation Hugoniot and discriminant $\Delta(s,\dot{s},\dot{y})$ for: (*b*1), $\dot{s}\lesssim\kappa(\dot{y})$; (*b*2), $\dot{s}=\dot{\kappa}$; (*b*3), $\dot{s}\gtrsim\dot{\kappa}$.

The straight line $y=y_x(\dot{s},\dot{y})$ belongs to the evaporation Hugoniot curve for $(\dot{s},\dot{y})\in\mathcal{E}$. On the other hand, for $(\dot{s},\dot{y})$ out of $\mathcal{E}$ the straight line $y=y_x(\dot{s},\dot{y})$ is an asymptote of the evaporation Hugoniot, as we will see in Lemmas 4.10 and 4.15. We have $-\delta_{gv}/\varrho_v\leqslant y_x(\dot{s},\dot{y})\leqslant 0$, therefore level $y_x(\dot{s},\dot{y})$ lies above the horizontal asymptote of the curve $\mathcal{E}_k$, see Definition 2.1, that is, we have $\mathsf{y}_r\equiv-(\mu_b+1)/\mu_{db}<-\delta_{gv}/\varrho_v\leq y_x(\dot{s},\dot{y})$ that leads to $(\varrho_g-\varrho_v)\,\mu_{db}<(\mu_b+1)\varrho_v$, *i.e.*, $\varrho_v>\varrho_g\,\mu_{db}/(\mu_d+1)$, which holds by Assumption 2.3.(b).

The intersection of $y=y_x(\dot{s},\dot{y})$ with the curve $\mathcal{E}_k$ occurs at the saturation value:

$$\dot{s}_x\equiv s_x(\dot{s},\dot{y})\equiv\dot{\Phi}/(\dot{\Phi}+\dot{\chi}). \tag{4.15}$$

For $(\dot{s},\dot{y})\in\mathcal{E}$ the saturation $s_x(\dot{s},\dot{y})$ takes the values:

$$s_x(0,\dot{y})=\tfrac{\mu_b}{\mu_b+1},\quad s_x(\kappa(\dot{y}),\dot{y})=\tfrac{\mu_b\varrho_v\varrho_g\dot{v}+\pi_2\varrho_b\varrho_d\dot{r}}{(\mu_b+1)\varrho_v\varrho_g\dot{v}+(\pi_2+\varrho_v)\varrho_b\varrho_d\dot{r}},\quad s_x(1,\dot{y})=\tfrac{\pi_2}{\pi_2+\varrho_v}. \tag{4.16}$$

The self-intersection of evaporation Hugoniot occurs at $(\dot{s}_x,\dot{y}_x)$; see Figs. 3.*a*/*e*/*i* again.

In the following lemma, we study the discriminant (4.10) of Eq. (4.8) for $(\dot{s},\dot{y})\in\mathcal{E}$. Then we will perturb $(\dot{s},\dot{y})$ away from $\mathcal{E}$; see Lemma 4.9 and Fig. 2.

LEMMA 4.8. Consider the discriminant $\Delta(s,\dot{s},\dot{y})$ in Eq. (4.10). We have:

(i) for $(\dot{s},\dot{y})\in\mathcal{E}$: $\Delta(s,\dot{s},\dot{y})$ is not a negative sixth order polynomial in s with three double roots, namely, $s=0$, $s=\dot{s}_x$ and $s=1$; see Eq. (4.15) and Fig. 2.b2;

(ii) at $s=1$: $\Delta(s,\dot{s},\dot{y})$ has a double root for all $(\dot{s},\dot{y})\in\mathcal{D}$ and it is upward concave.

PROOF OF LEMMA 4.8. (i) For $(\dot{s},\dot{y})\in\mathcal{E}$ we have $\dot{\beta}=\dot{\eta}=0$ as well as $x_1=x_2=x_3=0$ in Eq. (4.11b). Therefore we have $X_0=X_1=0$, $X_2=\dot{\Phi}^2$, $X_3=-2\,\dot{\Phi}(\dot{\Phi}+\dot{\chi})$, and $X_4=(\dot{\Phi}+\dot{\chi})^2$. Thus:

$Q(s;\dot{s},\dot{y})=s^2\left(\dot{\Phi}-(\dot{\Phi}+\dot{\chi})\,s\right)^2$ and $\Delta(s,\dot{s},\dot{y})=(\dot{\Phi}+\dot{\chi})\,s^2\left(\dot{s}_x-s\right)^2(1-s)^2$.

(ii) We have $Q(1;\dot{s},\dot{y})=\dot{\chi}^2-4\,\mu_{db}\,\dot{\eta}\,(\dot{\chi}+\delta_{bd}\,\dot{\beta})$, which is positive, as we will prove in Lemmas 4.11 and 4.14. Therefore, from Eq. (4.10), $s=1$ is a double root of Δ and the second derivative of Δ is also positive at $s=1$. □

From Lemma 4.8 we know that the discriminant $\Delta(s,\dot{s},\dot{y})$ for $(\dot{s},\dot{y})\in\mathcal{E}$ has three double roots, namely 0, $\dot{s}_x$ and 1– see bottom of Fig. 2.b2. In the next lemma we study $\Delta(s,\dot{s},\dot{y})$ for s close to $\dot{s}_x$ and $\dot{s}$ close to $\dot{s}=0$, $\dot{s}=\kappa(\dot{y})$, or $\dot{s}=1$; we keep $\dot{y}$ constant. That is, we are concerned with right states close to $\dot{s}_x$. For the left states we have three cases: close to $\dot{s}=0$, $\dot{s}=\kappa(\dot{y})$, or $\dot{s}=1$.

LEMMA 4.9. Consider $(\grave{s},\grave{y}) \in \mathcal{E}$, that is, $\grave{s}=0$, $\grave{s}=\kappa(\grave{y})$, or $\grave{s}=1$. For s close to $\grave{s}_x$, $a>0$, $b \gtrsim 0$, and $(\grave{s},\grave{y})$ such that:

(i) $\grave{s} \gtrsim 0$, then $\Delta(s,\grave{s},\grave{y}) \approx a\,(s-\grave{s}_x)^2 + b$, see bottom of Fig. 2.a;

(ii.a) $\grave{s} \lesssim \kappa(\grave{y})$, then $\Delta(s,\grave{s},\grave{y}) \approx a\,(s-\grave{s}_x)^2 + b$, see middle of Fig. 2.a and Fig. 2.b1;

(ii.b) $\grave{s} \gtrsim \kappa(\grave{y})$, then $\Delta(s,\grave{s},\grave{y}) \approx a\,(s-\grave{s}_x)^2 - b$, see middle of Fig. 2.a and Fig. 2.b3;

(iii) $\grave{s} \lesssim 1$, then $\Delta(s,\grave{s},\grave{y}) \approx a\,(s-\grave{s}_x)^2 - b$, see top of Fig. 2.a.

PROOF OF LEMMA 4.9. We need to examine three cases: (i) $\grave{s}$ close to 0; (ii) $\grave{s}$ close to $\kappa(\grave{y})$; (iii) $\grave{s}$ close to 1. Since $\Delta = Q\,\bar{s}^2$, we study Q instead of Δ. We denote the partial derivative with respect to s by dots, for instance, $\partial Q/\partial s \equiv \dot{Q}$; we denote by a prime the partial derivative with respect to $\grave{s}$, that is, $\partial Q/\partial \grave{s} = Q'$. The lemma holds since we have:

(i) $\dot{Q}(\grave{s}_x,0,\grave{y}) = \dot{Q}(\grave{s}_x,\kappa(\grave{y}),\grave{y}) = \dot{Q}(\grave{s}_x,1,\grave{y}) = 0$;

(ii) $\ddot{Q}(\grave{s}_x,0,\grave{y}) = \ddot{Q}(\grave{s}_x,\kappa(\grave{y}),\grave{y}) = \ddot{Q}(\grave{s}_x,1,\grave{y}) = 2\,\grave{\Phi}^2$;

(iii) $Q'(\grave{s}_x,0,\grave{y}) > 0$; $Q'(\grave{s}_x,\kappa(\grave{y}),\grave{y}) < 0$; $Q'(\grave{s}_x,1,\grave{y}) > 0$;

(iv) $Q'(\grave{s}_x;0,\grave{y}) = \big(4\,\varrho_v\varrho_g\grave{r}^2\grave{v}\mu_b^2\varrho_d\mu_{db}(\varrho_b\grave{g}\mu_b + \varrho_v\varrho_g\big)/(\mu_b+1)^3 > 0$;

(v) $Q'(\grave{s}_x;\kappa(\grave{y}),\grave{y}) = -\dfrac{4\,\mu_{db}(\varrho_g\grave{v}+\varrho_b\varrho_d\grave{r})(\varrho_v\varrho_g(\mu_b+1)\grave{v}+\varrho_b\varrho_d(\pi_2+\varrho_v)\grave{r})}{(\varrho_v^2\varrho_g^2\grave{v}+\varrho_b\varrho_v\varrho_g\pi_1\grave{r}+\mu_b\varrho_b\varrho_v\varrho_g\grave{g}\grave{v}+\varrho_b^2\varrho_d\pi_2\grave{r}\grave{g})(\grave{r}+1)^3} < 0$;

(vi) $Q'(\grave{s}_x;1,\grave{y}) = \big(4\varrho_d\varrho_b\varrho_v\mu_{db}\pi_1\pi_2^2(\varrho_v\varrho_g+\varrho_d\varrho_b\pi_2\grave{g})\big)\big/(\pi_2+\varrho_v)^3 > 0$. □

The discriminant at the origin is non-negative and vanishes if and only if $(\grave{s},\grave{y}) \in \mathcal{E}$; note that $Q(0,\grave{s},\grave{y})$ equals $X_0 = (\pi_3\,\grave{\beta})^2$.

See Fig. 2(b2): the discriminant Δ has three double roots and the evaporation Hugoniot has a self-intersection at $(\grave{s}_x,\grave{y}_x)$. Perturbing $\grave{s}$ to the left, see Fig. 2(b1), the discriminant is positive except for $s=1$, therefore there are two evaporation branches everywhere. On the other hand, perturbing $\grave{s}$ to the right, see Fig. 2(b3), the discriminant becomes negative close to 0 and $\grave{s}_x$, therefore some gaps on the evaporation branch arise. The following lemma is based on [18] and establishes the existence of four possible asymptotes to the evaporation Hugoniot.

LEMMA 4.10. Given a state $(\grave{s},\grave{y}) \in \mathcal{D}$, the evaporation Hugoniot from $(\grave{s},\grave{y})$ has at most four straight asymptotes. The candidates to asymptotes are:

(a) vertical asymptotes: (i) $s=1$ (multiplicity two) and

$$(ii)\quad s = -\delta_{bd}\,\grave{\beta}\,/\,\grave{\chi} \equiv s_a(\grave{s},\grave{y}) \equiv \grave{s}_a \tag{4.17}$$

(b) horizontal asymptotes: (i) $y = \mathsf{y}_\mathsf{r}$ and (ii) $y = y_x(\grave{s},\grave{y}) \equiv \grave{y}_x$.

PROOF OF LEMMA 4.10. In this proof we follow the notation and ideas of [18].

We write $\mathcal{Z}(s,y,\grave{s},\grave{y}) = \sum_{i=0}^{3}\sum_{j=0}^{2} z_{ij}\,s^i\,y^j$, where z_{ij} depend on $(\grave{s},\grave{y})$ and on model constants. We define the homogeneous polynomials of degree k

$$P_k(s,y) = \sum_{i+j=k} z_{ij}\,s^i\,y^j \;\text{ for }\; (i,j) \in \{0,3\}\times\{0,2\} \;\text{ and }\; k \in \{0,5\}.$$

First, we look for the possible asymptotes yielded by s^3: We have $P_5 = z_{32}\,s^3\,y^2 = z_{32}\,(a\,s+by)^3\,y^2$ where $a=1$, $b=0$. Also s^2 divides $P_4(s,y)$ and s divides $P_3(s,y)$, so we have $P_5 = s^3\,Q_5(s,y)$, $P_4 = s^2\,Q_4(s,y)$ and $P_3 = s\,Q_3(s,y)$ for appropriate Q's. The

possible asymptotes are $a\,s + b\,y = t_0$ where t_0 is a real root of the equation

$$t^3\,Q_5(0,-1) + t^2\,Q_4(0,-1) + t\,Q_3(0,-1) + P_2(0,-1) = 0. \tag{4.18}$$

We have $Q_5(0,-1) = z_{32}$, $Q_4(0,-1) = z_{22}$, $Q_3(0,-1) = z_{12}$ and $P_2(0,-1) = z_{02}$; so, Eq. (4.18) is also $\mathrm{A}(t) = 0$; see Eq. (4.8). Therefore, we have two possible asymptotes, $s = 1$ (double) and $s = -\delta_{bd}\,\grave{\beta}/(\grave{\alpha} + \varrho_v\,\grave{\gamma})$; see Eq. (4.6a); $t = 1$ is a double root of Eq. (4.18).

Now, we look for the possible asymptotes yielded by y^2: we have $P_5 = z_{32}\,s^3\,y^2 = z_{32}\,s^3\,(a\,s + by)^2$, where $a = 0$, $b = 1$. As y divides $P_4(s,y)$ we have $P_5 = y^2 Q_5(s,y)$ and $P_4 = y\,Q_4(s,y)$ for appropriate Q's. The possible asymptotes are $a\,s + b\,y = t_0$ where t_0 is a real root of the equation

$$t^2\,Q_5(1,0) + t\,Q_4(1,0) + P_3(1,0) = 0. \tag{4.19}$$

We have $Q_5(1,0) = z_{32}$, $Q_4(1,0) = z_{31}$ and $P_3(1,0) = z_{30}$; so Eq. (4.19) is also $\mathrm{L}(t) = 0$; see Eq. (4.9). Therefore, we have two possible asymptotes, one is $r(y)+1 = 0$, *i.e.*, $y = \mathsf{y_r}$ (see Definition 2.1) and the other is $y = -\delta_{gv}\grave{\gamma}\,/\,\grave{\chi} \equiv y_x(\grave{s},\grave{y})$; see Eq. (4.7a). □

The candidates to vertical asymptotes given in lemma 4.10 are actually asymptotes. The location of the vertical asymptote at $\grave{s}_a$ is studied in the next lemma.

Lemma 4.11. The function $\grave{s}_a$, Eq. (4.17), vanishes for $(\grave{s},\grave{y}) \in \mathcal{E}$ and for $\grave{y} = 0$. For $\grave{y} > 0$ the function $\grave{s}_a$:

(i) is positive for $\grave{s} \in (0, \kappa(\grave{y}))$, that is, for $(\grave{s},\grave{y}) \in \mathcal{R}_L$;

(ii) is negative for $\grave{s} \in (\kappa(\grave{y}), 1)$, that is, for $(\grave{s},\grave{y}) \in \mathcal{R}_R$;

(iii) satisfies $-\frac{\delta_{bd}\,\varrho_g}{\varrho_b\,\varrho_d}\,\frac{1}{\mu_b+1} \le \grave{s}_a \le \frac{\delta_{bd}}{\varrho_b}\,\frac{\mu_d}{\mu_d+1}$.

Proof of Lemma 4.11. The roots of the function $\grave{s}_a \equiv s_a(\grave{s},\grave{y})$ (see Lemma 4.10) are the same as the roots of $\grave{\beta}$; see Eq. (3.14a.ii). The denominators of $\grave{s}_a$ and δ_{bd} are strictly positive, therefore $-\grave{\beta}$ determines the sign of $\grave{s}_a$. Since ϱ_v and ϱ_g are positive, the sign of $\grave{s}_a$ is the same as that of

$$-\grave{\beta} = -\varrho_v\,\varrho_g\,\grave{s}\,\grave{\bar{s}}\,\grave{y}\,\mathsf{K}(\grave{s},\grave{y}) = \varrho_v\,\varrho_g\,\grave{y}\,\grave{s}\,(\grave{s}-1)\,\big((\grave{r}+1)\,\grave{s} - \grave{r}\big). \tag{4.20}$$

Therefore, if $\grave{y} = 0$, then $\grave{s}_a$ vanishes for all $\grave{s} \in [0,1]$. For $\grave{y} > 0$, then $\grave{s}_a$ is cubic in $\grave{s}$ and has three distinct roots, 0, $\kappa(\grave{y})$, and 1, and positive leading coefficient, so $\grave{s}_a$ is positive for $\grave{s} \in (0,\kappa(\grave{y}))$ and negative for $\grave{s} \in (\kappa(\grave{y}), 1)$. Then (i) and (ii) hold.

In order to prove (iii), we substitute Eqs. (3.14a) and (3.14b.i) in Eq. (4.17), so

$$\grave{s}_a = -\frac{\delta_{bd}\,\grave{\beta}}{\grave{\chi}} = -\frac{\delta_{bd}\,\varrho_v\,\varrho_g\,\grave{s}\,\grave{\bar{s}}\,\grave{y}\,(\grave{s} - \grave{r}\,\grave{\bar{s}})}{\varrho_v\,\varrho_g\,\grave{\bar{s}}^2\,\grave{r}\,\grave{v} + \varrho_v\,\varrho_b\,\varrho_d\,\grave{s}^2}.$$

For $(\grave{s},\grave{y}) \in \mathcal{R}_L$ we have $\grave{s}_a > 0$, $-\grave{r}\,\grave{\bar{s}} < \grave{s} - \grave{r}\,\grave{\bar{s}} < 0$ and $0 \le \grave{\gamma}$; then

$$\grave{s}_a \le \frac{\delta_{bd}\,\varrho_v\,\varrho_g\,\grave{s}\,\grave{\bar{s}}\,\grave{y}\,\grave{r}\,\grave{\bar{s}}}{\varrho_v\,\varrho_g\,\grave{\bar{s}}^2\,\grave{r}\,\grave{v}} = \frac{\delta_{bd}\,\grave{s}\,\grave{y}}{\grave{v}} = \frac{\delta_{bd}\,\grave{y}\,\grave{s}}{\delta_{bd}\,\grave{y} + \varrho_d} \le \frac{\delta_{bd}}{\varrho_b}\,\grave{s} \le \frac{\delta_{bd}}{\varrho_b}\,\frac{\mu_d}{\mu_d+1}. \tag{4.21}$$

For $(\grave{s},\grave{y}) \in \mathcal{R}_L$ we have $\grave{s}_a < 0$, $0 < \grave{s} - \grave{r}\,\grave{\bar{s}} < \grave{s}$ and $0 \le \grave{\alpha}$; then

$$\grave{s}_a \ge -\frac{\delta_{bd}\,\varrho_v\,\varrho_g\,\grave{s}^2\,\grave{\bar{s}}\,\grave{y}}{\varrho_v\,\varrho_b\,\varrho_d\,\grave{s}^2} \ge -\frac{\delta_{bd}\,\varrho_g}{\varrho_b\,\varrho_d}\,\grave{\bar{s}} \ge -\frac{\delta_{bd}\,\varrho_g}{\varrho_b\,\varrho_d}\,\frac{1}{\mu_b+1}. \tag{4.22}$$

So the lemma holds. □

COROLLARY 4.12. From Eqs. (4.21) and (4.22) we have ($\grave{\bar{s}}_a = 1 - \grave{s}_a$):

$$(i)\ \frac{\varrho_b + \mu_d\,\varrho_d}{\varrho_b + \mu_d\,\varrho_b} \le \grave{\bar{s}}_a \quad \text{and} \quad (ii)\ \grave{\bar{s}}_a \le 1 + \frac{\delta_{bd}\,\varrho_g}{\varrho_b\,\varrho_d}\,\frac{1}{\mu_b+1}. \tag{4.23}$$

We have already established the existence and location of the vertical asymptote $s = \grave{s}_a$; now we classify it according to Lemma A.2.

LEMMA 4.13. Consider $(\grave{s}, \grave{y}) \in \mathcal{D} \setminus \mathcal{E}$. The asymptote $s = \grave{s}_a$ is (see Definition A.1):
(i) Type VR for $0 < \grave{s} < \kappa(\grave{y})$, *i.e.*, for $(\grave{s}, \grave{y}) \in \mathcal{R}_L$;
(ii) Type VL for $\kappa(\grave{y}) < \grave{s} < 1$, *i.e.*, for $(\grave{s}, \grave{y}) \in \mathcal{R}_R$.

PROOF OF LEMMA 4.13. By the definition of $\grave{s}_a$ we have $\mathrm{A}(\grave{s}_a) = 0$; see Eqs. (4.6a) and (4.17). Following Lemma A.2, we need to calculate the sign of $\mathrm{A}'(\grave{s}_a)\,\mathrm{B}(\grave{s}_a)$, where the prime means $\mathrm{d}/\mathrm{d}s$. A straight calculation shows that: $\mathrm{A}'(\grave{s}_a) = \mu_{db}\,(1 - \grave{s}_a)^2\,\grave{\chi} > 0$.

From Eqs. (4.6b) and (4.17) we have:

$$\begin{aligned}\mathrm{B}(\grave{s}_a) &= -\grave{\bar{s}}_a\left(\grave{\chi}\,\grave{s}_a^2 - \left(\mu_b\,\grave{\alpha} + (2\,\mu_b\,\varrho_v - \pi_2)\grave{\gamma}\right)\grave{s}_a\,\grave{\bar{s}}_a - (\pi_3 + 2\,\varrho_d\,\mu_{db})\,\grave{\beta}\,\grave{\bar{s}}_a\right)\\ &= \left(\mu_{db}\,\grave{\Pi}\,\grave{\bar{s}}_a - \delta_{bd}^2\,\grave{\beta}\right)\grave{\beta}\,\grave{\bar{s}}_a \,/\, \grave{\chi}. \end{aligned}\tag{4.24}$$

From Corollary 4.12, we have $0 < \grave{\bar{s}}_a$, so the following factors in Eq. (4.24) are positive: $\grave{\bar{s}}_a \,/\, \grave{\chi} > 0$ and $\mu_{db}\,\grave{\bar{s}}_a(\varrho_d\,\grave{\alpha} + \pi_1\,\grave{\gamma}) > 0$.

For $\grave{\beta} < 0$, that is, for $\grave{s}_a > 0$ iff $(\grave{s}, \grave{y}) \in \mathcal{R}_L$ we get $\mathrm{B}(\grave{s}_a) < 0$ and so the first part of the lemma holds.

For $\grave{\beta} > 0$, that is, for $\grave{s}_a < 0$ iff $(\grave{s}, \grave{y}) \in \mathcal{R}_R$ the sign of $\mathrm{B}(\grave{s}_a)$ depends on Assumption 2.3(c), which ensures that $\mu_{db}\,\grave{\bar{s}}_a(\varrho_d\,\grave{\alpha} + \pi_1\,\grave{\gamma}) - \delta_{bd}^2\,\grave{\beta}$ is positive:

$$\mu_{db}\,\grave{\Pi}\,\grave{\bar{s}}_a - \delta_{bd}^2\,\grave{\beta} > 0 \Leftrightarrow \mu_d > \mu_b + \delta_{bd}^2\,\grave{\beta}\,/(\grave{\Pi}\,\grave{\bar{s}}_a). \tag{4.25}$$

We need an upper bound for $\delta_{bd}^2\,\grave{\beta}\,/(\grave{\Pi}\,\grave{\bar{s}}_a) = \delta_{bd}^2\,\grave{\beta}/\grave{\bar{s}}_a(\varrho_d\,\grave{\alpha} + \pi_1\,\grave{\gamma})$:

$$\frac{\delta_{bd}^2\,\grave{\beta}}{\grave{\bar{s}}_a(\varrho_d\,\grave{\alpha} + \pi_1\,\grave{\gamma})} < \frac{\delta_{bd}^2\,\grave{\beta}}{\grave{\bar{s}}_a\,\pi_1\,\grave{\gamma}} = \frac{\delta_{bd}^2\,\varrho_v\,\varrho_g\,\grave{s}\,\grave{\bar{s}}\,\grave{y}\,(\grave{s} - r(\grave{y})\,\grave{\bar{s}})}{\grave{\bar{s}}_a\,\pi_1\,\varrho_b\,\varrho_d\,\grave{s}^2} < \frac{\delta_{bd}^2\,\varrho_v\,\varrho_g\,\grave{s}^2\,\grave{\bar{s}}\,\grave{y}}{\grave{\bar{s}}_a\,\pi_1\,\varrho_b\,\varrho_d\,\grave{s}^2};$$

then from Eqs. (3.23), (4.23.i) we have:

$$\frac{\delta_{bd}^2\,\grave{\beta}}{\grave{\bar{s}}_a(\varrho_d\,\grave{\alpha} + \pi_1\,\grave{\gamma})} < \frac{\delta_{bd}^2\,\varrho_v\,\varrho_g\,\grave{\bar{s}}}{\grave{\bar{s}}_a\,\pi_1\,\varrho_b\,\varrho_d} < \frac{\delta_{bd}^2\,\varrho_v\,\varrho_g}{(\varrho_b + \mu_d\,\varrho_d)\,\pi_1\,\varrho_d} = \mathfrak{U}_1.$$

Then $\mu_d > \mu_b + \mathfrak{U}_1$ ensures that Eq. (4.24) holds; furthermore $\mathrm{sign}(B(\grave{s}_a)) = \mathrm{sign}(\grave{\beta})$. □

For $(\grave{s}, \grave{y})$ lying on curve $\mathcal{E}$; see Fig. 3.c, $s = 0$ is an asymptote as well as a solution for $\mathcal{Z}(s, y, \grave{s}, \grave{y}) = 0$, as we show in Lemma 4.7.

In the next lemma we classify the asymptote located at $s = 1$ according to Lemma A.3.

LEMMA 4.14. Consider $(\grave{s}, \grave{y}) \in \mathcal{D} \setminus \mathcal{E}$ and the straight line $s = 1$. There is no solution of Eq. (4.8) on $s = 1$ so the straight line is a branch separatrix. The straight line is an asymptote of (see Definition A.1): (i) Type VUD for $\grave{s} < \kappa(\grave{y})$, *i.e.*, $(\grave{s}, \grave{y}) \in \mathcal{R}_L$; (ii) Type VLL for $\grave{s} > \kappa(\grave{y})$, *i.e.*, $(\grave{s}, \grave{y}) \in \mathcal{R}_R$.

PROOF OF LEMMA 4.14. We have $\mathrm{A}(1)=0$, $\mathrm{A}'(1)=0$, $\mathrm{A}''(1)=2\,\mu_{db}\,(\grave{\chi}+\delta_{bd}\,\grave{\beta})$, or, alternatively, $\mathrm{A}''(1)=2\,\mu_{db}\,\grave{\chi}\,\grave{\tilde{s}}_a>0$; note that we are studding $s=1$; we are using $\grave{\tilde{s}}_a$ here only because we know that $\grave{\tilde{s}}_a$ is positive. A straightforward computation shows that $\mathrm{B}(1)=0$, $\mathrm{B}'(1)=\grave{\chi}>0$ and $\mathrm{C}(1)=\grave{\eta}$.

Trivially there is no solution of Eq. (4.8) on $s=1$: $\mathrm{A}(1)\,y^2+\mathrm{B}(1)\,y+\mathrm{C}(1)=0$ iff $\grave{\eta}=0$; and $\grave{\eta}=0$ if and only if $(\grave{s},\grave{y})\in\mathcal{E}$. In order to study the asymptote type we need to know $\mathrm{sign}(\mathrm{A}''(1)\,\mathrm{C}(1))$; see Lemma A.3. We have $\mathrm{sign}(\mathrm{A}''(1)\,\mathrm{C}(1))=\mathrm{sign}(\mathrm{C}(1))=\mathrm{sign}(\grave{\eta})=\mathrm{sign}(\mathsf{K}(\grave{s},\grave{y}))$, so the sign of $\mathrm{A}''(1)\,\mathrm{C}(1)$ is negative for $(\grave{s},\grave{y})\in\mathcal{R}_1\cup\mathcal{R}_2\cup\mathcal{R}_3$ and positive for $(\grave{s},\grave{y})\in\mathcal{R}_4\cup\mathcal{R}_5$. Then, statement (i) holds. The second part of the lemma holds since (i) $\mathrm{sign}(\mathrm{A}''(1)\,\mathrm{C}(1))>0$; (ii) $\mathrm{sign}(\mathrm{B}'(1)\,\mathrm{C}(1))>0$; (iii) Assumption (c).ii ensures that $2\,\mathrm{A}''(1)\,\mathrm{C}(1)<\mathrm{B}^2(1)$ (see below).

We need to prove that $2\,\mathrm{A}''(1)\,\mathrm{C}(1)<B^2(1)$:

$$\mathrm{B}'(1)^2-2\,\mathrm{A}''(1)\,\mathrm{C}(1)=\grave{\chi}^2-4\,\mu_{db}\,\grave{\chi}\,\grave{\tilde{s}}_a\grave{\eta}>0\Leftrightarrow\grave{\chi}-4\,\mu_{db}\,\grave{\tilde{s}}_a\grave{\eta}>0\Leftrightarrow\mu_d<\mu_b+\tfrac{\grave{\chi}}{4\,\grave{\tilde{s}}_a\grave{\eta}}.$$

We need a lower bound for $\grave{\chi}\,/\,(4\,\grave{\tilde{s}}_a\grave{\eta})$ for $(s,y)\in\mathcal{R}_R$, so we use Eqs. (3.23), (4.23.i)

$$\frac{\grave{\chi}}{4\,\grave{\tilde{s}}_a\grave{\eta}}>\frac{\frac{\varrho_v\,\varrho_d\mu_b(\varrho_v+\varrho_b\mu_b)}{(\mu_b+1)^2}}{4\left(1+\frac{\delta_{bd}\,\varrho_g}{\varrho_b\,\varrho_d}\,\frac{1}{\mu_b+1}\right)\left(\frac{\varrho_b\,\varrho_d\,\varrho_g}{4}\,\frac{1}{\mu_b+1}\right)}=\frac{\varrho_v\,\varrho_d\,(\varrho_v+\varrho_b\,\mu_b)}{\varrho_g(\varrho_d\,\varrho_b\,\mu_b+\varrho_d\,\varrho_b+\varrho_v\,\delta_{bd})}\,\mu_b=\mathfrak{U}_2.$$

□

We remark that $4\,\mu_{db}\,\grave{\chi}\,\grave{\tilde{s}}_a\grave{\eta}=\mu_{db}\,\grave{\eta}\,(\grave{\chi}+\delta_{bd}\,\grave{\beta})$, therefore, here and in Lemma 4.8 the issue is the same, the discriminant must be non-negative close to $s=1$.

LEMMA 4.15. Consider $(\grave{s},\grave{y})\notin\mathcal{E}$ and $\grave{y}\neq0$. The asymptote $y=y_x(\grave{s},\grave{y})$ contains no solution, so it is a Hugoniot branch separatrix.

PROOF OF LEMMA 4.15. For $y=y_x(\grave{s},\grave{y})$ we trivially have $\mathrm{L}(y)=0$; see Eqs. (4.7a) and (4.14). Straightforward calculations shows that Eq. (4.9) reduces to a second degree equation with discriminant:

$$\boldsymbol{\Delta}\big(y_x(\grave{s},\grave{y})\big)=-4\,\grave{\Pi}\,\grave{\Phi}\,\grave{\beta}\,\grave{\eta}\,/\,\grave{\chi}^2. \tag{4.26}$$

(See Definition 2.4.) For $(\grave{s},\grave{y})$ out of $\mathcal{E}$ and $\grave{y}\neq0$ we have $\grave{\beta}\neq0$, $\grave{\eta}\neq0$ and $\mathrm{sign}(\grave{\beta})=\mathrm{sign}(\grave{\eta})$; then $\boldsymbol{\Delta}\big(y_x(\grave{s},\grave{y})\big)<0$ and there are no solutions of $\mathcal{H}(s,y_x(\grave{s},\grave{y}),\grave{s},\grave{y})=0$. □

LEMMA 4.16. Consider $\grave{W}=(\grave{s},\grave{y},\grave{u})$ and $W\in\mathscr{H}(\grave{W})$. Therefore, the classification of the shock between $\grave{W}$ and W is independent of the choice of $\grave{u}>0$.

PROOF OF LEMMA 4.16. For $W\neq\grave{W}$ outside the self-intersection Hugoniot locus, matrix M of Eq. (4.3) has rank two, therefore the solution is spanned by a vector, say (α,β,γ); that is, $(u,\grave{u},\varphi\,\sigma)=k\,(\alpha,\beta,\gamma)$ for some $k\in\mathbb{R}$. Given some $\grave{u}>0$ we have $k=\grave{u}/\beta$, $u=\grave{u}\,\alpha/\beta$, and $\sigma=\grave{u}\,\gamma/(\varphi\beta)$ with $\beta\neq0$. Therefore, shock speed σ and u are proportional to $\grave{u}$ (for $\grave{u}>0$).

The left eigenvalues are proportional to $\grave{u}$, as follows from Eq. (3.2). In the same fashion, right eigenvalues are proportional to u. Since u is itself proportional to $\grave{u}$, then right eigenvalues are also proportional to $\grave{u}$. The shock classification depends on left and

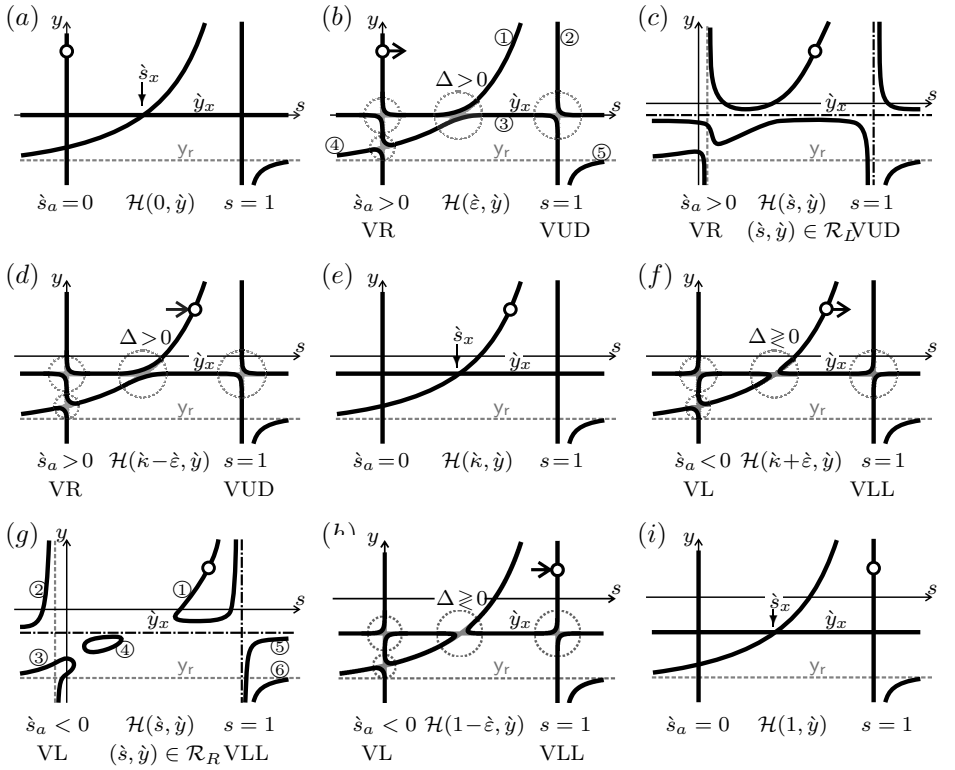

FIG. 3. **The evaporation Hugoniot**. White circle: state $(\grave{s},\grave{y})$; solid black line: evaporation Hugoniot; gray dashed line: non-separatrix asymptote; black dashed-dotted line: separatrix asymptote.

right eigenvalues as well as on shock speed, which are all proportional to $\grave{u}$, therefore, the shock classification does not depend on $\grave{u}$. □

4.2. *Description of the behavior of the evaporation Hugoniot.* Now we are able to describe how the evaporation Hugoniot behaves. For $\grave{s}=0$ Lemma 4.7 establishes that $\mathcal{Z}=0$ is formed by the straight lines $s=0$, $s=1$ and $y=0$ together with curve $\mathcal{E}_k$; see Fig. 3.a. The discriminant of $\mathcal{Z}$ vanishes at $s=0$, $s=\grave{s}_x$ and $s=1$ (see Lemma 4.9). Therefore, $\mathcal{Z}$ at $\grave{s}_x(0,\grave{y})$ has a double root and the evaporation Hugoniot has a self-intersection (between the curve $\mathcal{E}_k$ and the straight line $y=\grave{y}_x$).

Moving $(\grave{s},\grave{y})$ toward $\mathcal{R}_L$ (see Fig. 3.b) two vertical asymptotes replace the vertical lines: (i) an asymptote of type VR at $s=\grave{s}_a>0$ and another one of type VUD at $s=1$. The horizontal line is replaced by a horizontal separatrix asymptote at level $y=\grave{y}_x$. As stated in Lemma 4.9, the double root at $\grave{s}_x$ splits into two branches, since $\Delta(s,\grave{s},\grave{y})>0$ close to $(s=\grave{s}_x,\grave{s}=0)$. We number the five branches of Fig. 3.b with circled numbers. The branch ① lies above $y=\grave{y}_x$ and between $s=\grave{s}_a$ and $s=1$. All other branches lie below $y=\grave{y}_x$ except branch ② which lies on right of $s=1$. Therefore, the only branch which intersects $\mathcal{D}$ is branch ①.

For $(\grave{s}, \grave{y}) \in \mathcal{R}_L$; see Fig. 3.c, the evaporation Hugoniot displays the same behavior as in Fig. 3.b. As $(\grave{s}, \grave{y})$ approaches curve $\mathcal{E}_k$ (see Fig. 3.d): (i) $\grave{s}_a$ is still positive but gets closer to zero again; (ii) Δ is still positive but becomes closer to zero near $\grave{s}_x$. Then, when $(\grave{s}, \grave{y}) \in \mathcal{E}_k$ we have again curve $\mathcal{E}_k$ together with two vertical lines, $s = 0$ and $s = 1$, and a horizontal one now at a negative level $y = \grave{y}_x$; see Fig. 3.e.

Moving $(\grave{s}, \grave{y})$ toward $\mathcal{R}_R$ (see Fig. 3.f) two vertical asymptotes replace the vertical lines: (i) an asymptote of type VL at $s = \grave{s}_a < 0$ (examine Fig. 3.g to see the details as branch ③ tends to $-\infty$) and another of type VLL at $s = 1$. The horizontal line is replaced by a horizontal separatrix asymptote at level $y = \grave{y}_x$. From Lemma 4.9, we know that Δ changes sign leading to two folds close to $\grave{s}_x$.

For $(\grave{s}, \grave{y}) \in \mathcal{R}_R$; see Fig. 3.g, the evaporation Hugoniot is formed by six branches. The branch ① lies above $y = \grave{y}_x$ and between $s = \grave{s}_a$ and $s = 1$. All other branches lie below $y = \grave{y}_x$ except branch ②, which lies on the left of $\grave{s}_a < 0$. Therefore, the only branch that intersects $\mathcal{D}$ is branch ①. As $\grave{s}$ approaches 1 all the branches glue together again at $\mathcal{E}_k$ and at three lines, $s = 0$, $s = 1$ and $y = \grave{y}_x$; see Figs. 3.h and 3.i.

We conclude that there are only two generic configurations for the evaporation Hugoniot curve; see Figs. 3.c and 3.g.

4.3. *Rankine-Hugoniot configurations.* From the previous results, we get:

THEOREM 4.17. The part of evaporation Hugoniot that intersects $\mathcal{D}$ has two stable configurations:

(1) for $(\grave{s}, \grave{y}) \in \mathcal{R}_L$; see Figs. 3.c, the evaporation Hugoniot has two vertical asymptotes, at $s = \grave{s}_a < \grave{s}$ and $s = 1$, and a minimum that may occur for negative y;
(2) for $(\grave{s}, \grave{y}) \in \mathcal{R}_R$; see Figs. 3.g, the evaporation Hugoniot has a double vertical asymptote at $s = 1$, and a minimum that may occur for negative y.

On the other hand, for $(\grave{s}, \grave{y}) \in \mathcal{E}$ the evaporation Hugoniot is formed by the set $\mathcal{E}$ itself and by the straight line $y = \grave{y}_x$; see Fig. 4.a/e/i and Figs. 3.a/e/i; this configuration is unstable under small perturbations of $(\grave{s}, \grave{y})$.

The Hugoniot locus is the union of the saturation and evaporation branches. These two branches intersect twice except for $(\grave{s}, \grave{y}) \in \mathcal{C} = \mathcal{I}_e^m \cup \mathcal{I}_e^M$ where the minimum of the evaporation Hugoniot occurs at $(\grave{s}, \grave{y})$; see Fig. 4.c/g.

5. Riemann solution. In this paper we use the wave curve method to solve Riemann problems; see [1, 12, 13]. The following theorem (see [25]) applies away from self-intersection Hugoniot locus.

THEOREM 5.1 (Bethe-Wendroff). Assume that W belongs to the Hugoniot curve from $\grave{W}$ and that $l_i(G(W) - G(\grave{W})) \neq 0$. Then the following are equivalent: (i) $\mathrm{d}\sigma(W, \grave{W}) = 0$; (ii) $\sigma(W, \grave{W}) = \lambda_i(W)$, for some i. Cases (i)/(ii) hold; then $\mathrm{d}W = r_i(W)$, that is, the Hugoniot curve is tangent to the i-rarefaction.

The Bethe-Wendroff theorem determines the states where a shock curve is followed by a rarefaction curve of same family without an intermediate state, namely, right characteristic shocks. Rarefaction curves cannot be followed by shock curves; although,

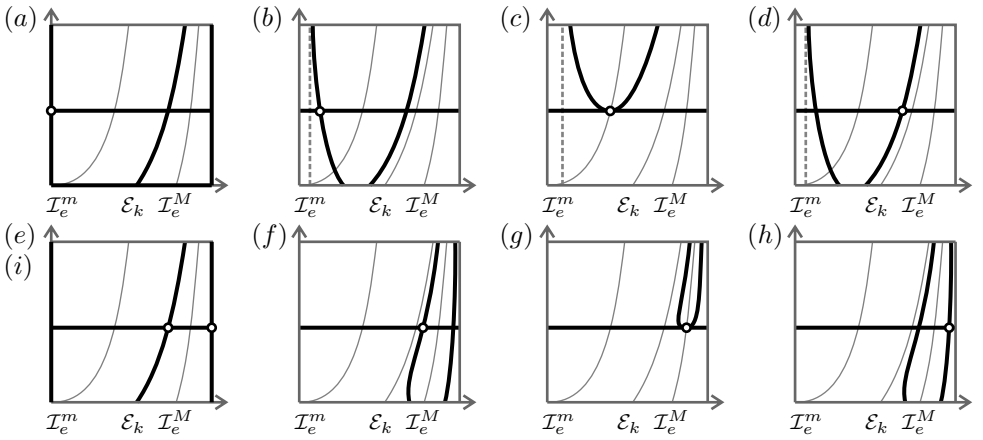

FIG. 4. **The Hugoniot locus**. White circle: (a) $(\grave{s}, \grave{y}) \in \mathcal{E}_0$; (b) $(\grave{s}, \grave{y}) \in \mathcal{R}_1$; (c) $(\grave{s}, \grave{y}) \in \mathcal{I}_e^m \subset \mathcal{C}$; (d) $(\grave{s}, \grave{y}) \in \mathcal{R}_2 \cup \mathcal{R}_3$; (e) $(\grave{s}, \grave{y}) \in \mathcal{E}_k \subset \mathcal{I}_e$; (f) $(\grave{s}, \grave{y}) \in \mathcal{R}_4$; (g) $(\grave{s}, \grave{y}) \in \mathcal{I}_e^M \subset \mathcal{C}$; (h) $(\grave{s}, \grave{y}) \in \mathcal{R}_5$; (i) $(\grave{s}, \grave{y}) \in \mathcal{E}_1$. Black solid curve and line: Hugoniot. Gray dashed line: Hugoniot's asymptote. Gray solid thin curves: evaporation inflection.

rarefactions waves may be followed by left characteristic shock waves without intermediate states. In this case, the rarefaction curve is followed by a composite curve that is an envelope of Hugoniot curves, as stated in [16]. Here we present a short version of the theorem appropriate for non-trivial accumulation, which ignores the admissibility and compatibility issues. For details on how this theorem allows one to study non-local solutions see [15] and [16].

THEOREM 5.2. Let $\grave{W}$ be a family of states that lie on an i-rarefaction curve away from i-Inflection locus. Let W be a correspondent family of states on the Hugoniot from $\grave{W}$ such that $G(\grave{W}) \neq G(W)$ and $\sigma(\grave{W}, W) = \lambda_i(\grave{W}) \neq \lambda_j(W)$ hold for every pair $(\grave{W}, W)$, some i and all j; the shock from $\grave{W}$ to W is left characteristic away from double contact. Then, the family of states W is the envelope of the curves $\mathscr{H}(\grave{W})$.

PROOF OF LEMMA 5.2. The Hugoniot from $\grave{W}$ is the set of W for which there is a speed σ such that $F(W) - F(\grave{W}) - \sigma(G(W) - G(\grave{W})) = 0$; differentiating and setting $\sigma = \lambda_i(\grave{W})$ we get (taking G, DF and DG at W and $\grave{\lambda}_i$, $\grave{G}$ at $\grave{W}$):

$$\big(DF - \grave{\lambda}_i DG\big)\mathrm{d}W - \big(G - \grave{G}\big)\mathrm{d}\sigma = 0; \tag{5.1}$$

since $\grave{\lambda}_i \neq \lambda_j(W)$, for all j, we have full rank $DF - \grave{\lambda}_i DG$ and non-vertical well-defined direction $\mathrm{d}W$ stated by Eq. (5.1).

The family W is given by $F(W) - F(\grave{W}) - \lambda_i(\grave{W})(G(W) - G(\grave{W})) = 0$; differentiating we get (taking $D\grave{F}$, $D\grave{G}$ at $\grave{W}$):

$$(DF - \grave{\lambda}_i DG)\mathrm{d}W - (D\grave{F} - \grave{\lambda}_i D\grave{G})\mathrm{d}\grave{W} - (G - \grave{G})\nabla\grave{\lambda}_i \mathrm{d}\grave{W} = 0; \tag{5.2}$$

moving $\grave{W}$ on i-rarefaction with vector speed given by any eigenvector associated to $\grave{\lambda}_i$, say $\grave{r}_i$, we get $(DF - \grave{\lambda}_i DG)\mathrm{d}W - (G - \grave{G})\nabla\grave{\lambda}_i \cdot \grave{r}_i = 0$; we have $\nabla\grave{\lambda}_i \cdot \grave{r}_i \neq 0$ since $\grave{W}$ does not belong to i-Inflection, then Eq. (5.1) and (5.2) define the same direction. □

TABLE 2. Classification of Hugoniot curve depending on scaled shock $\hat{\sigma}$ and scaled characteristic speeds $\check{\lambda}_i = \check{\lambda}_i(\grave{s}, \grave{y})$ and $\hat{\lambda}_i = \hat{\lambda}_i(s, y)$.

Symbol	Speed relationships	Symbol	Speed relationships
$+\pm$	$\check{\lambda}_2 < \hat{\sigma}, \quad \hat{\lambda}_1 < \hat{\sigma} < \hat{\lambda}_2$	$\pm-$	$\check{\lambda}_1 < \hat{\sigma} < \check{\lambda}_2, \quad \hat{\sigma} < \hat{\lambda}_1$
$\pm+$	$\check{\lambda}_1 < \hat{\sigma} < \check{\lambda}_2, \quad \hat{\lambda}_2 < \hat{\sigma}$	$-\pm$	$\hat{\sigma} < \check{\lambda}_1, \quad \hat{\lambda}_1 < \hat{\sigma} < \hat{\lambda}_2$
$++$	$\check{\lambda}_2 < \hat{\sigma}, \quad \hat{\lambda}_2 < \hat{\sigma}$	$--$	$\hat{\sigma} < \check{\lambda}_1, \quad \hat{\sigma} < \hat{\lambda}_1$
$-+$	$\hat{\sigma} < \check{\lambda}_1, \quad \hat{\lambda}_1 < \hat{\sigma}$	$\pm\pm$	$\check{\lambda}_1 < \hat{\sigma} < \check{\lambda}_2, \quad \hat{\lambda}_1 < \hat{\sigma} < \hat{\lambda}_2$
$+-$	$\check{\lambda}_2 < \hat{\sigma}, \quad \hat{\sigma} < \hat{\lambda}_1$		

5.1. *Classification of discontinuities.* The classification of a Hugoniot curve in three variables usually depends on three eigenvalues and shock speed. However, here the Hugoniot is classified based on just two characteristic speeds.

In this section, we classify each point (s, y) in the projected Hugoniot locus from $(\grave{s}, \grave{y})$ according to the relation between the scaled shock speed $\hat{\sigma}$ and the scaled characteristic speeds $\check{\lambda}_i = \check{\lambda}_i(\grave{s}, \grave{y})$ and $\hat{\lambda}_i = \hat{\lambda}_i(s, y)$. We use the classification scheme from Table 2 with the symbols in the first column related to the signs of $\hat{\sigma} - \check{\lambda}_i$ and $\hat{\sigma} - \hat{\lambda}_i$; see also Figs. 6.a. (For two negative signs: "$-$"; for one negative and the other positive: "$\pm$"; for two positive signs: "$+$".) On the saturation Hugoniot (where $y = \grave{y}$), the shock classification may be studied geometrically using $\hat{\lambda}_s$ and $\hat{\lambda}_e$ (see Fig. 1) as well as $\hat{\sigma}$; the speed $\hat{\sigma}$ is given by the slope of the secant through $(\grave{s}, \grave{y})$ and (s, y). This leads to speed relationships similar to those found in the Buckley-Leverett solution (see [2]). See Fig. 6.b and, for instance, the white circle on $\mathcal{R}_1$ (the highest). The white circle represents $(\grave{s}, \grave{y})$ and then the shocks from $(\grave{s}, \grave{y})$ to states on its left are 1-shocks.

The evaporation Hugoniot has a *minimum*, that is, it has a point tangent to $(1, 0)$. For $(\grave{s}, \grave{y})$ away from the evaporation Inflection locus, at that minimum the Bethe-Wendroff applies and we have: $\hat{\sigma} = \hat{\lambda}_s$ and $\dot{\sigma} = 0$. At the doubly-sonic $\hat{\lambda}_e$ the Bethe-Wendroff theorem is not applicable, since it occurs at the self-intersection locus (see Lemma 4.6). For $(\grave{s}, \grave{y})$ on the evaporation Inflection, the evaporation Hugoniot has a minimum at

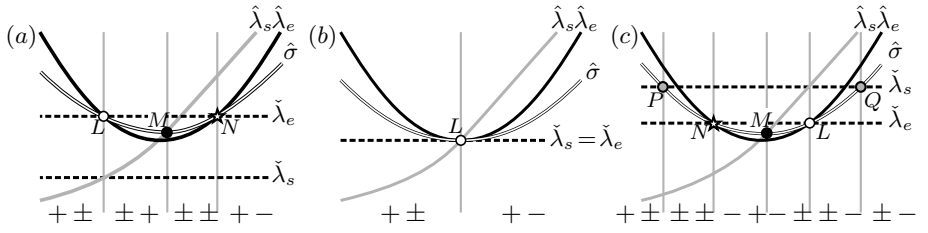

FIG. 5. The classification of the evaporation Hugoniot curve close to $\mathcal{I}_e^m$. **White circles**: left state $L \equiv (\grave{s}, \grave{y})$; **stars**: self-intersection state, N (shock speed equals both left and right-eigenvalue); **black circles**: shock speed equals right-eigenvalue, M; **gray circles**: shock speed equals left-eigenvalue, P and Q; (a) Classification for $L \in \mathcal{R}_1$; (b) Classification for $L \in \mathcal{I}_e^m$; (c) Classification for $L \in \mathcal{R}_2 \cup \mathcal{R}_3$.

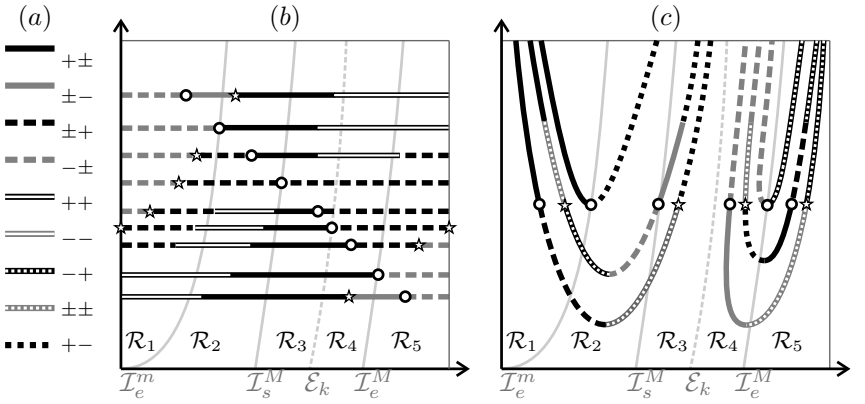

FIG. 6. White circles: left state; stars: self-intersection of projected Hugoniot. (a) Caption for Hugoniot Classification. (b) Classification of saturation Hugoniot; (c) Classification of evaporation Hugoniot.

$(\grave{s}, \grave{y})$. The classification of the evaporation Hugoniot based on Fig. 5 we also check numerically.

At $\mathcal{I}_e^m$ the eigenvalues $\hat{\lambda}_s$ and $\hat{\lambda}_e$ are equal, $\hat{\lambda}_e$ has a minimum and $\hat{\lambda}_s$ increases as s increases; see Fig 5.(b).

Consider $L \equiv (\grave{s}, \grave{y}) \in \mathcal{I}_e^m$; see Fig 5.(b). The shock speed $\hat{\sigma}$ is larger than both left eigenvalues $\check{\lambda}_s$ and $\check{\lambda}_e$. For (s, y) on the right part of evaporation Hugoniot we have $\hat{\sigma}$ smaller than both right eigenvalues $\hat{\lambda}_s$ and $\hat{\lambda}_e$. For (s, y) on the left part of evaporation Hugoniot, we have $\hat{\sigma}$ larger than $\hat{\lambda}_s$ and smaller than $\hat{\lambda}_e$. There are just two types of discontinuities: $+\pm$ and $+-$.

Consider $L \equiv (\grave{s}, \grave{y}) \in \mathcal{R}_1$, as in the Fig 5.(a). The speed $\hat{\sigma}$ has the same value as the eigenvalues at three points, the white circle $L \equiv (\grave{s}, \grave{y})$, the black circle M (at the minimum) and the star N (at the self-intersection). There are four classifications as in the figure.

Consider $L \equiv (\grave{s}, \grave{y}) \in \mathcal{R}_2 \cup \mathcal{R}_3$; see Fig 5.(c). The speed $\hat{\sigma}$ has the same value as the eigenvalues at five points, the white circle $L \equiv (\grave{s}, \grave{y})$, the black circle M (at the minimum), the star N (at the self-intersection), as well as at the gray circles P and Q where the shock is left characteristic. There are six classifications as in the figure.

The eigenvalue $\hat{\lambda}_e$ has a maximum at $\mathcal{I}_e^M$ while $\hat{\lambda}_s$ decreases as s increases. The classification is similar to the previous one. Namely, drawing Fig. 5 upside down we get the interchange signs $+$ with $-$ (while $\pm$ keeps unchanged). Based on numerical evidence, we conjecture that classification is the same for $(\grave{s}, \grave{y})$ away from the Inflection.

5.2. *Solution diagrams.* We present the solution diagrams for $(\grave{s}, \grave{y})$ in $\mathcal{R}_1$, $\mathcal{I}_e^m$, $\mathcal{R}_2$, $\mathcal{R}_3$, $\mathcal{E}_k$, $\mathcal{R}_4$, $\mathcal{I}_e^M$, and $\mathcal{R}_5$, respectively on Figs. 8.a to 11.b. In the diagrams, the left state is depicted as a white circle. (The right state may be any point of the domain.)

In our kind of construction (left-to-right choice), the solution of a Riemann problem is parametrized by a sequence of wave curves, which necessarily goes from the left state L to the right state R. However, in order to obtain the wave sequence from our figures it is easier to start at R and proceed backwards to L. (Despite which the waves are still

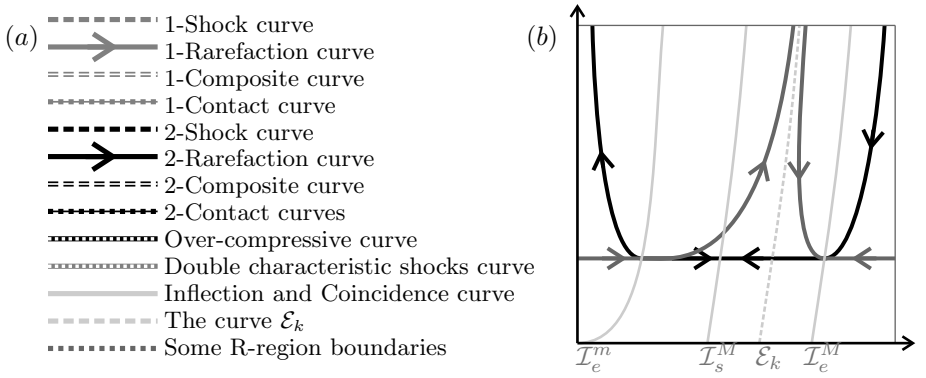

FIG. 7. (a) Graphical representation of the thirteen wave-curves from the solution. (b) Rarefaction curves in L-regions $\mathcal{R}_1$to $\mathcal{R}_5$.

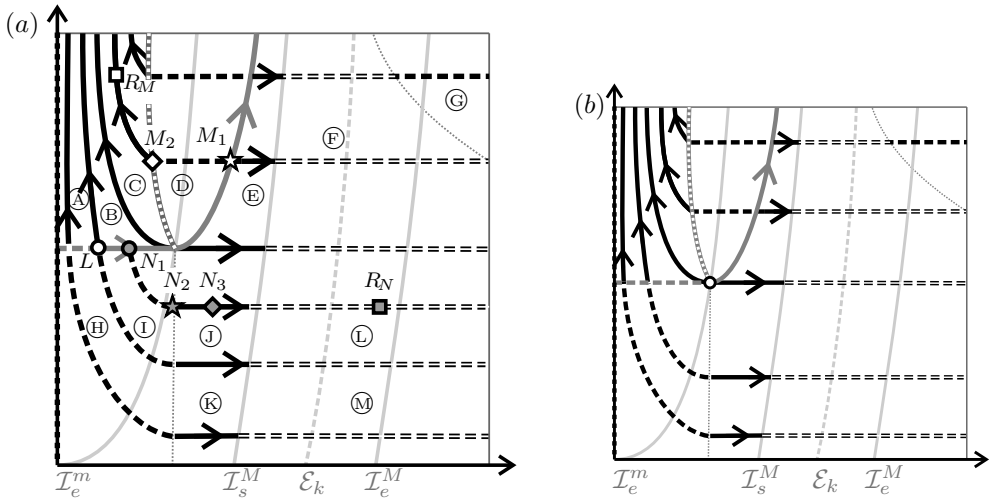

FIG. 8. White circles represent $(\dot{s}, \dot{y})$. Solution for: (a) $(\dot{s}, \dot{y}) \in \mathcal{R}_1$; (b) $(\dot{s}, \dot{y}) \in \mathcal{I}_e^m$.

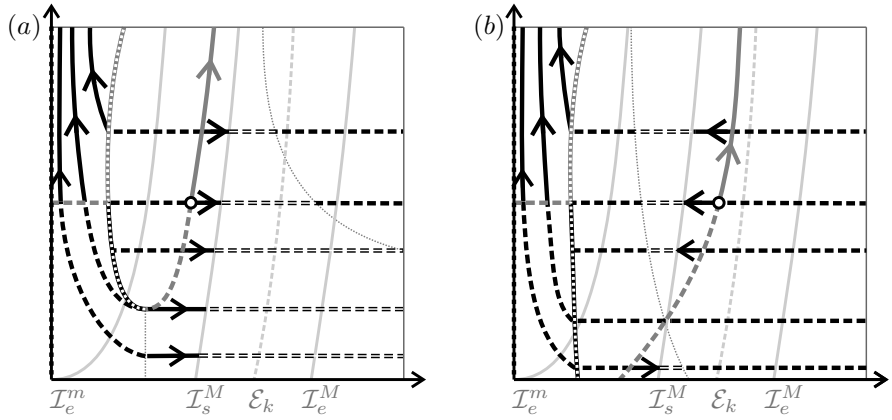

FIG. 9. White circles represent $(\dot{s}, \dot{y})$. Solution for: (a) $(\dot{s}, \dot{y}) \in \mathcal{R}_2$; (b) $(\dot{s}, \dot{y}) \in \mathcal{R}_3$.

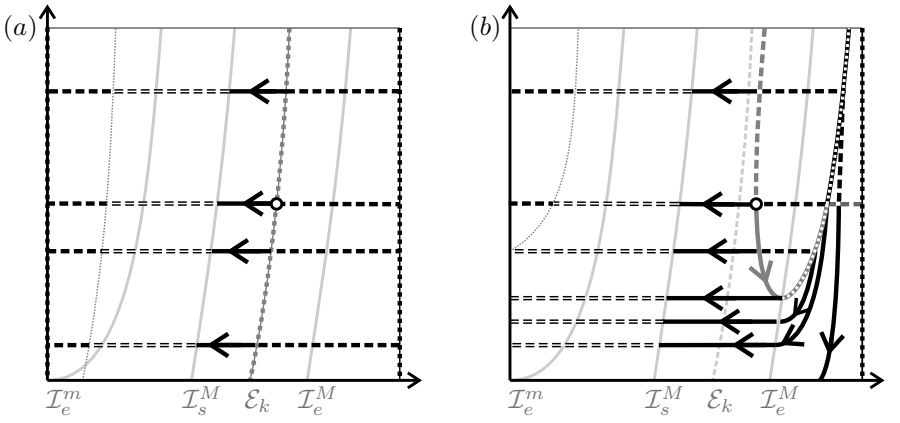

FIG. 10. White circles represent $(\grave{s}, \grave{y})$. Solution for: (a) $(\grave{s}, \grave{y}) \in \mathcal{E}_k$; (b) $(\grave{s}, \grave{y}) \in \mathcal{R}_4$.

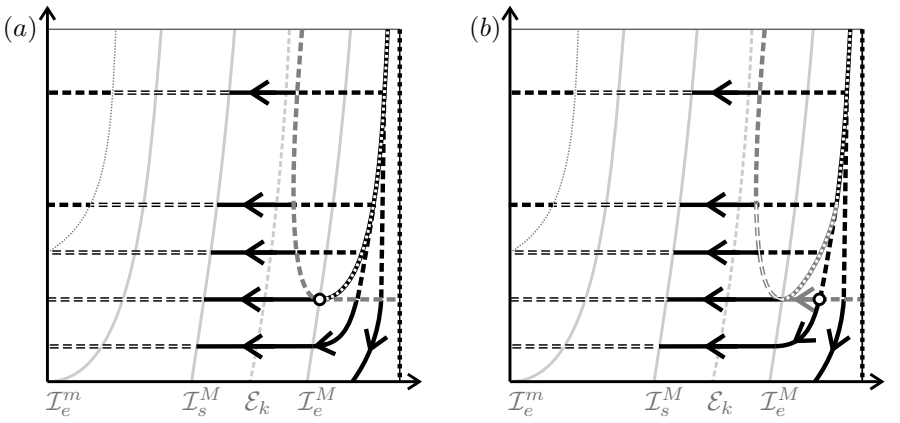

FIG. 11. White circles represent $(\grave{s}, \grave{y})$. Solution for: (a) $(\grave{s}, \grave{y}) \in \mathcal{I}_e^M$; (b) $(\grave{s}, \grave{y}) \in \mathcal{R}_5$.

forward waves in the sense given in [14].) We need: (I) to locate all 1-wave curves from L (1-shock, 1-rarefaction, and 1-composite curves; see Fig. 7.a for conventions on graphical representations); (II) to identify the 2-wave curves through R and their intersection with the curves located in (I).

We show how to apply this methodology to find the solution for $L \in \mathcal{R}_1$, illustrated in Fig. 8.a. Any point in Fig. 8.a represents a possible R, while L is the small white circle. (I) The 1-wave curves from L are marked in solid and dashed dark gray; (II) The intersections are explained in the two examples that follow.

EXAMPLE 5.3. Consider the right state R_M in the R-region © depicted as a white square in the left top part of Fig. 8.a. Following backwards through the 2-rarefaction curve we reach the white diamond M_2 on the double characteristic curve (gray railway), then the 2-shock curve connects the diamond with the white star M_2 on the 1-rarefaction from L. From M_1 we go backwards to L. Therefore, the solution of this Riemann problem comprises three waves without intermediate state (as in [22] and [17]): (i) a 1-rarefaction

from left state to L to M_1; (ii) a double-characteristic shock (see Lemma 4.4) from M_1 to M_2; and (iii) a 2-rarefaction from M_2 to R_M.

EXAMPLE 5.4. Consider the right state R_N on R-region Ⓛ depicted as a gray square in Fig. 8.a (southeast from the center of the picture). Following backwards through the black curve we reach a gray circle N_1 on the 1-rarefaction from L. However, R_N lies on a 2-composite curve, therefore there exist a state on preceding 2-rarefaction, say N_3, such that the shock from N_3 to R_N is right characteristic (see Theorem 5.2). The 2-rarefactions do not connect N_1 to N_3; then there is a right characteristic 2-shock from N_1 to N_2 to joins the 2-rarefaction (as conditions of Theorem 5.1 are satisfied). Therefore, the solution of this Riemann problem comprises two wave groups: (i) a 1-rarefaction from left state to L to N_1; (ii) a 2-wave group without intermediate states: (ii.a) a right characteristic 2-shock from N_1 to N_2; (ii.b) a 2-rarefaction from N_2 to N_3; (ii.c) and a left characteristic 2-shock from N_3 to R_N.

For $(\grave{s}, \grave{y}) \in \mathcal{R}_1$, we show the wave sequence for the thirteen R-regions labeled from Ⓐ to Ⓜ, and we use the wave nomenclature of Table 1 in [15]. We have:

(A) S_1R_1	(B) R_1R_2	(C) $R_1{}'S'_OR_2$	(D) R_1S_2	(E) R_1R_2
(F) $R_1R_2{}'S_2$	(G) R_1S_2	(H) S_1S_2	(I) R_1S_2	(J) $R_1S'_2R_2$
(K) $S_1S'_2R_2$	(L) $R_1S'_2R_2{}'S_2$	(M) $S_1S'_2R_2{}'S_2$.		

We have 1-composite curves only for $(\grave{s}, \grave{y})$ in $\mathcal{R}_5$ (see double dashed gray line in Fig. 11.b); these curves are envelopes of Hugoniot evaporation branches. The family of over-compressive shocks fail to be an envelope since the double-characteristic shock occur on self-intersection Hugoniot locus; see Lemma 4.6.

The solutions depend L^1_{loc} continuously on left and right states.

Appendix A. Solutions of one parameter quadratic and cubic equations. Consider $p(s, y) = a(s)\, y^2 + b(s)\, y + c(s) = 0$, quadratic equation in y where a, b, c are smooth functions depending on the parameter s. The discriminant is $\Delta(s) = b^2(s) - 4\, a(s)\, c(s)$. For non-vanishing denominator and non-negative discriminant we define:

$$\mathsf{B}_{\pm}(s) = -2\, c(s) \big/ \big(b(s) \pm \sqrt{\Delta(s)}\big). \tag{A.1}$$

If $a(s) = 0$ we have $\sqrt{\Delta(s)} = |b(s)|$, then the denominator of (A.1) does not vanish in the following cases: (i) if $b(s) > 0$, we have $\mathsf{B}_+(s) = -c(s)/b(s)$; (ii) if $b(s) < 0$, we have $\mathsf{B}_-(s) = -c(s)/b(s)$. The real solutions of $p = 0$, written as functions of s, are $\mathsf{B}_{\pm}(s)$.

We define two types of asymptotes that will be used in Lemma A.2 and play an important role in proving the bifurcation of the evaporation Hugoniot (see Lemma 4.13.).

DEFINITION A.1. Let $f : \mathbb{R} \to \mathbb{R}$ be a function of s which graph has a vertical asymptote at s_0. We say the asymptote is type:

- VL if $\lim\limits_{s \to s_0^{\pm}} f(s) = \mp\infty$; see Fig. 12.*a*;
- VR if $\lim\limits_{s \to s_0^{\pm}} f(s) = \pm\infty$; see Fig. 12.*b*;
- VU if $\lim\limits_{s \to s_0^{\pm}} f(s) = +\infty$; see Fig. 12.*c*;
- VD if $\lim\limits_{s \to s_0^{\pm}} f(s) = -\infty$; see Fig. 12.*c*.

(The capital letters stand for: V-vertical, L-left, R-right, D-down, and U-up.)

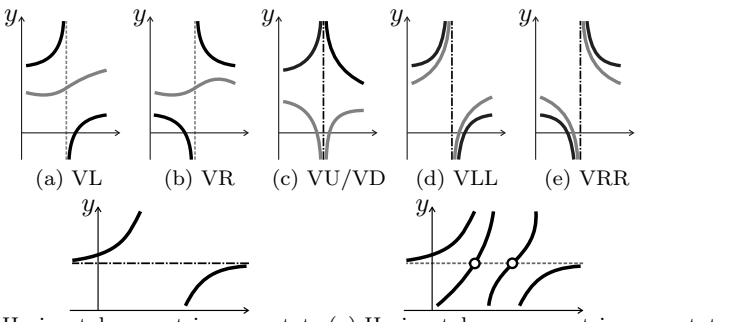

FIG. 12. Solid lines gray and black: the branches $\mathsf{B}_{\pm}$; black dash-doted lines: separatrix asymptotes; gray dashed lines: non-separatrix asymptotes. (a) Type VL, Lemma A.2; (b) Type VR, Lemma A.2; (c) Type VU and VD, Lemma A.3.1; (d) Type VLL, Lemma A.3.2; (e) Type VRR, Lemma A.3.3; (f) Horizontal separatrix asymptote; (g) Horizontal non-separatrix asymptote.

We represent the derivative $\mathrm{d}/\mathrm{d}s$ using a prime and for the evaluations at s_0 we simplify the notation in such a way: $a(s_0) \equiv a_0$, $a'(s_0) \equiv a'_0$, etc. In the following lemmas we study the solutions of p close to a point where a vanishes.

LEMMA A.2. For $a_0 = 0$, $a'_0 \neq 0$, $b_0 \neq 0$, $c_0 \neq 0$ and $\sigma = \operatorname{sign}(b)$ we have:

(1) the graph of $\mathsf{B}_\sigma(s)$ is a non-vertical smooth curve close to $(s_0, \mathsf{B}_\sigma(s_0))$;
(2) the graph of $\mathsf{B}_{-\sigma}(s)$ has an asymptote at $s = s_0$ of:
    (i) type VL if $a'_0\, b_0 > 0$, see Fig. 12.a; (ii) type VR if $a'_0\, b_0 < 0$; see Fig. 12.b.

A more degenerate case, $a_0 = 0$, is treated in the next lemma.

LEMMA A.3. For $a_0 = 0$, $a'_0 = 0$, $a''_0 \neq 0$, $b_0 = 0$, $b'_0 \neq 0$ and $c_0 \neq 0$ both solutions of $p(s, y) = 0$, B_+ and B_-, have a branch separatrix asymptote at s_0 of:

(1) Type VUD, one is type VU and the other is type VD, if $a''_0\, c_0 < 0$ (see Fig. 12.c);
(2) Type VLL, both type VL, if $0 < 2\, a''_0\, c_0 < (b'_0)^2$ and $a_0\, b'_0 > 0$ (see Fig. 12.d);
(3) Type VRR, both type VR, if $0 < 2\, a''_0\, c_0 < (b'_0)^2$ and $a_0\, b'_0 < 0$ (see Fig. 12.e).

Acknowledgments. We thank Ricardo Barros for pointing us to the paper of J. Nunemacher, [18], and Nuno Luzia for some suggestions for simplifying the analysis.

REFERENCES

[1] Arthur V. Azevedo, Aparecido J. de Souza, Frederico Furtado, Dan Marchesin, and Bradley Plohr, *The solution by the wave curve method of three-phase flow in virgin reservoirs*, Transp. Porous Media **83** (2010), no. 1, 99–125, DOI 10.1007/s11242-009-9508-9. MR2646866

[2] S.E. Buckley and M.C. Leverett, *Mechanism of fluid displacements in sands*, Transactions of the AIME **146** (1942), 107–116.

[3] Olav Dahl, Thormod Johansen, Aslak Tveito, and Ragnar Winther, *Multicomponent chromatography in a two phase environment*, SIAM J. Appl. Math. **52** (1992), no. 1, 65–104, DOI 10.1137/0152005. MR1148319

[4] J.M. Dumore, J. Hagoort, and A.S. Risseeuw, *An analytical model for one-dimensional, three-component condensing and vaporizing gas drives*, SPEJ **24** (1984), 169 – 179.
[5] Eli L. Isaacson and J. Blake Temple, *Analysis of a singular hyperbolic system of conservation laws*, J. Differential Equations **65** (1986), no. 2, 250–268, DOI 10.1016/0022-0396(86)90037-9. MR861520
[6] Thormod Johansen and Ragnar Winther, *The solution of the Riemann problem for a hyperbolic system of conservation laws modeling polymer flooding*, SIAM J. Math. Anal. **19** (1988), no. 3, 541–566, DOI 10.1137/0519039. MR937469
[7] Barbara L. Keyfitz and Herbert C. Kranzer, *A system of nonstrictly hyperbolic conservation laws arising in elasticity theory*, Arch. Rational Mech. Anal. **72** (1979/80), no. 3, 219–241, DOI 10.1007/BF00281590. MR549642
[8] Barbara L. Keyfitz and Herbert C. Kranzer, *The Riemann problem for a class of hyperbolic conservation laws exhibiting a parabolic degeneracy*, J. Differential Equations **47** (1983), no. 1, 35–65, DOI 10.1016/0022-0396(83)90027-X. MR684449
[9] L.W. Lake, *Enhanced oil recovery*, Prentice Hall, 1989.
[10] Wanderson Lambert and Dan Marchesin, *The Riemann problem for multiphase flows in porous media with mass transfer between phases*, J. Hyperbolic Differ. Equ. **6** (2009), no. 4, 725–751, DOI 10.1142/S0219891609001988. MR2604254
[11] Wanderson Lambert, Dan Marchesin, and Johannes Bruining, *The Riemann solution for the injection of steam and nitrogen in a porous medium*, Transp. Porous Media **81** (2010), no. 3, 505–526, DOI 10.1007/s11242-009-9419-9. MR2599978
[12] P. D. Lax, *Hyperbolic systems of conservation laws. II*, Comm. Pure Appl. Math. **10** (1957), 537–566, DOI 10.1002/cpa.3160100406. MR0093653
[13] Tai Ping Liu, *The Riemann problem for general* 2×2 *conservation laws*, Trans. Amer. Math. Soc. **199** (1974), 89–112, DOI 10.2307/1996875. MR0367472
[14] Arthur V. Azevedo, Cesar S. Eschenazi, Dan Marchesin, and Carlos F. B. Palmeira, *Topological resolution of Riemann problems for pairs of conservation laws*, Quart. Appl. Math. **68** (2010), no. 2, 375–393, DOI 10.1090/S0033-569X-10-01154-7. MR2663005
[15] V. Matos, A. V. Azevedo, J. C. Da Mota, and D. Marchesin, *Bifurcation under parameter change of Riemann solutions for nonstrictly hyperbolic systems*, Z. Angew. Math. Phys. **66** (2015), no. 4, 1413–1452, DOI 10.1007/s00033-014-0469-7. MR3377695
[16] Vítor Matos and Dan Marchesin, *Large viscous solutions for small data in systems of conservation laws that change type*, J. Hyperbolic Differ. Equ. **5** (2008), no. 2, 257–278, DOI 10.1142/S0219891608001477. MR2419998
[17] Vitor Matos, Julio D. Silva, and Dan Marchesin, *Loss of hyperbolicity changes the number of wave groups in Riemann problems*, Bull. Braz. Math. Soc. (N.S.) **47** (2016), no. 2, 545–559, DOI 10.1007/s00574-016-0168-4. MR3514420
[18] Jeffrey Nunemacher, *Asymptotes, Cubic Curves, and the Projective Plane*, Math. Mag. **72** (1999), no. 3, 183–192. MR1573393
[19] O. A. Oleĭnik, *On the uniqueness of the generalized solution of the Cauchy problem for a nonlinear system of equations occurring in mechanics* (Russian), Uspehi Mat. Nauk (N.S.) **12** (1957), no. 6(78), 169–176. MR0094543
[20] Stephen Schecter, Dan Marchesin, and Bradley J. Plohr, *Structurally stable Riemann solutions*, J. Differential Equations **126** (1996), no. 2, 303–354, DOI 10.1006/jdeq.1996.0053. MR1383980
[21] Stephen Schecter, Bradley J. Plohr, and Dan Marchesin, *Classification of codimension-one Riemann solutions*, J. Dynam. Differential Equations **13** (2001), no. 3, 523–588, DOI 10.1023/A:1016634307145. MR1845094
[22] Julio Daniel Silva and Dan Marchesin, *Riemann solutions without an intermediate constant state for a system of two conservation laws*, J. Differential Equations **256** (2014), no. 4, 1295–1316, DOI 10.1016/j.jde.2013.10.005. MR3145758
[23] Joel Smoller, *Shock waves and reaction-diffusion equations*, 2nd ed., Grundlehren der Mathematischen Wissenschaften [Fundamental Principles of Mathematical Sciences], vol. 258, Springer-Verlag, New York, 1994. MR1301779
[24] W.J. Todd, M.R.; Longstaff, *The development, testing, and application of a numerical simulator for predicting miscible flood performance*, Journal of Petroleum Technology **24** (1972), 874–882.
[25] Burton Wendroff, *The Riemann problem for materials with nonconvex equations of state. I. Isentropic flow*, J. Math. Anal. Appl. **38** (1972), 454–466, DOI 10.1016/0022-247X(72)90103-5. MR0328387